THE JOURNAL OF BIOLOGICAL CHEMISTRY VOL. 287, NO. 38, pp. 31905–31919, September 14, 2012

Generation of *N*-Acylphosphatidylethanolamine by Members of the Phospholipase A/Acyltransferase (PLA/AT) Family*

Received for publication, April 2, 2012, and in revised form, July 18, 2012 Published, JBC Papers in Press, July 23, 2012, DOI 10.1074/jbc.M112.368712

Toru Uyama[‡], Natsuki Ikematsu[§], Manami Inoue[§], Naoki Shinohara[‡], Xing-Hua Jin[‡¶], Kazuhito Tsuboi[‡], Takeharu Tonai[‖], Akira Tokumura[§], and Natsuo Ueda[‡1]

From the [‡]Department of Biochemistry, Kagawa University School of Medicine, 1750-1 Ikenobe, Miki, Kagawa 761-0793, Japan, the [§]Institute of Health Biosciences, University of Tokushima Graduate School, Tokushima 770-8505, Japan, the [¶]Department of Chemistry, Qiqihar Medical University, Qiqihar 161006, China, and the [‖]Department of Orthopedic Surgery and Clinical Research Institute, National Zentsuji Hospital, Zentsuji, Kagawa 765-0001, Japan

Background: The mammalian enzymes that form *N*-acylphosphatidylethanolamines (NAPEs), precursors of bioactive *N*-acylethanolamines, are poorly understood.
Results: PLA/AT family proteins, previously known as tumor suppressors, catalyzed *N*-acylation of phosphatidylethanolamine, and their overexpression in animal cells remarkably increased endogenous levels of NAPEs.
Conclusion: These proteins may function as NAPE-forming enzymes *in vivo*.
Significance: Our results may contribute to a better understanding of the regulatory mechanisms of *N*-acylethanolamine levels.

Bioactive *N*-acylethanolamines (NAEs), including *N*-palmitoylethanolamine, *N*-oleoylethanolamine, and *N*-arachidonoylethanolamine (anandamide), are formed from membrane glycerophospholipids in animal tissues. The pathway is initiated by *N*-acylation of phosphatidylethanolamine to form *N*-acylphosphatidylethanolamine (NAPE). Despite the physiological importance of this reaction, the enzyme responsible, *N*-acyltransferase, remains molecularly uncharacterized. We recently demonstrated that all five members of the HRAS-like suppressor tumor family are phospholipid-metabolizing enzymes with *N*-acyltransferase activity and are renamed HRASLS1–5 as phospholipase A/acyltransferase (PLA/AT)-1–5. However, it was poorly understood whether these proteins were involved in the formation of NAPE in living cells. In the present studies, we first show that COS-7 cells transiently expressing recombinant PLA/AT-1, -2, -4, or -5, and HEK293 cells stably expressing PLA/AT-2 generated significant amounts of [^{14}C]NAPE and [^{14}C]NAE when cells were metabolically labeled with [^{14}C]ethanolamine. Second, as analyzed by liquid chromatography-tandem mass spectrometry, the stable expression of PLA/AT-2 in cells remarkably increased endogenous levels of NAPEs and NAEs with various *N*-acyl species. Third, when NAPE-hydrolyzing phospholipase D was additionally expressed in PLA/AT-2-expressing cells, accumulating NAPE was efficiently converted to NAE. We also found that PLA/AT-2 was partly responsible for NAPE formation in HeLa cells that endogenously express PLA/AT-2. These results suggest that PLA/AT family proteins may produce NAPEs serving as precursors of bioactive NAEs *in vivo*.

Ethanolamides of different long-chain fatty acids constitute a class of naturally occurring lipid molecules and are collectively referred to as *N*-acylethanolamines (NAEs)[2] (1, 2). NAEs show a wide variety of biological activities depending on their acyl chains, and these activities are based on their abilities to bind to and activate specific receptors. In particular, *N*-arachidonoylethanolamine, also known as anandamide, has attracted much attention as an endogenous ligand for cannabinoid receptors (3) and for transient receptor potential vanilloid type-1 (TRPV1) (4). *N*-Palmitoylethanolamine and *N*-oleoylethanolamine have been documented as an anti-inflammatory and analgesic substance (5, 6) and appetite-suppressing substance (7), respectively, through peroxisome proliferator-activated receptor (PPAR) α (8, 9). *N*-Oleoylethanolamine was also reported to be an agonist of TRPV1 (10) and GPR119 (11).

NAE is biosynthesized from membrane glycerophospholipids by two steps of enzyme reactions (Fig. 1) (12, 13). The first step of the NAE-biosynthesizing pathway is the formation of *N*-acylphosphatidylethanolamine (NAPE) by transferring an acyl chain from the *sn*-1 position of glycerophospholipid to the amino group of phosphatidylethanolamine (PE). Although it has been established that membrane-bound Ca^{2+}-dependent *N*-acyltransferase (Ca-NAT) catalyzes this reaction in the brain (14–16), the enzyme has not been purified or cloned. The sec-

* This study was supported by grants-in-aid for scientific research from the Ministry of Education, Culture, Sports, Science, and Technology of Japan (to T. U. and K. T.), the Japan Society for the Promotion of Science (to N. U.), Kagawa University Faculty of Medicine Specially Promoted Research Fund 2010 (to T. U.), Fund for Kagawa University Young Scientists 2011 (to T. U. and K. T.), grants from the Ichiro Kanehara Foundation (to T. U.), the Sumitomo Foundation (to T. U.), the Uehara Memorial Foundation (to T. U.), and the Suzuken Memorial Foundation (to K. T.).
[1] To whom correspondence should be addressed. Tel.: 81-87-891-2102; Fax: 81-87-891-2105; E-mail: nueda@med.kagawa-u.ac.jp.

[2] The abbreviations used are: NAE, *N*-acylethanolamine; Ca-NAT, Ca^{2+}-dependent *N*-acyltransferase; FAAH, fatty acid amide hydrolase; GP-NAE, glycerophospho-*N*-acylethanolamine; iNAT, Ca^{2+}-independent *N*-acyltransferase; NAAA, *N*-acylethanolamine-hydrolyzing acid amidase; NAPE, *N*-acylphosphatidylethanolamine; NAPE-PLD, *N*-acylphosphatidylethanolamine-hydrolyzing phospholipase D; PC, phosphatidylcholine; PE, phosphatidylethanolamine; PLA, phospholipase A; PLA/AT, phospholipase A/acyltransferase; PMA, phorbol-12-myristate-13-acetate; pNAPE, *N*-acylated plasmenylethanolamine.

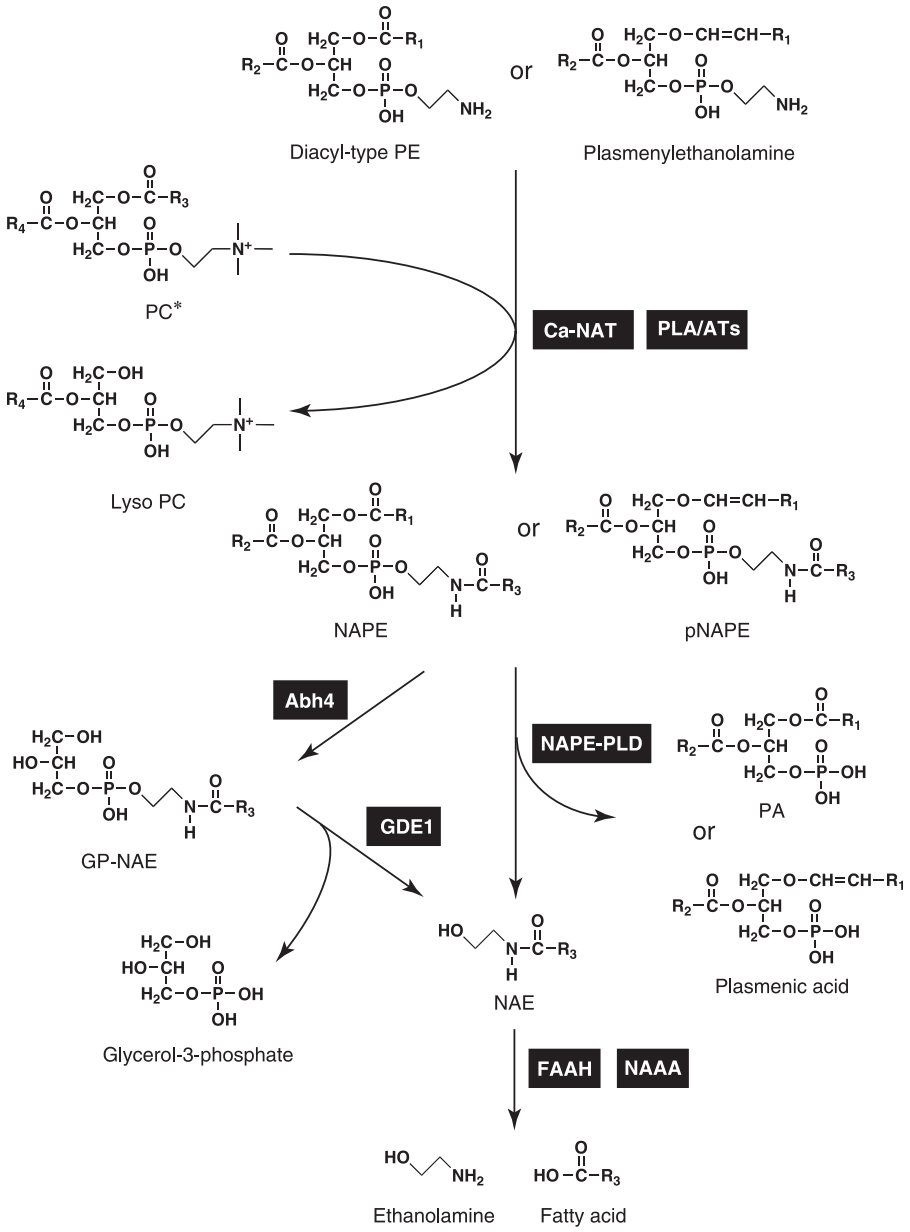

FIGURE 1. **Major biosynthetic and degradative pathways of NAPE and pNAPE.** *, PC is a representative acyl donor phospholipid. *Abh4*, α/β-hydrolase 4; *GDE1*, glycerophosphodiesterase 1; *PA*, phosphatidic acid.

ond step is the hydrolysis of NAPE to NAE by NAPE-hydrolyzing phospholipase D (NAPE-PLD) (17). Alternative pathways independent of NAPE-PLD are also known (18–20). As a major degradative pathway of NAE, the hydrolysis of NAE to fatty acid and ethanolamine is catalyzed by membrane-bound fatty acid amide hydrolase (FAAH) or lysosomal NAE-hydrolyzing acid amidase (NAAA) (Fig. 1) (12, 21, 22). Recent studies using knock-out mice and specific inhibitors revealed that these NAE-hydrolyzing enzymes are promising targets for the development of therapeutic drugs (6, 23).

The HRAS-like suppressor family (also known as the *H-rev107* family) consists of tumor suppressor genes negatively regulating the activity of oncogene Ras (16, 24–27). In human beings, five members (*HRASLS1–5*) belong to this family. Recently, we demonstrated that the gene products of all five members possess phospholipase $A_{1/2}$ ($PLA_{1/2}$) activity, which releases fatty acid from the *sn*-1 or *sn*-2 position of glycerophospholipid, and *O*-acyltransferase activity, which transfers an acyl group from glycerophospholipid to the hydroxyl group of lysophospholipid (28–31). Based on these phospholipid-metabolizing activities, we proposed to designate the gene products of *HRASLS1–5* as phospholipase A/acyltransferase-1–5 (PLA/AT-1–5), respectively (31). We will use these new names throughout this report.

We also found that these proteins have *N*-acyltransferase activity for the generation of NAPE. In particular, PLA/AT-5 (known as Ca^{2+}-independent *N*-acyltransferase, iNAT) (16, 28), PLA/AT-2 (known as HRASLS2) (30), and PLA/AT-1 (known as A-C1) (31) showed relatively high *N*-acyltransferase activities. However, based on their Ca^{2+} independency and other properties, we concluded that these proteins were different from the known Ca-NAT (16, 28, 30, 31). In a preliminary

experiment, we detected a [^{14}C]NAPE-like compound in PLA/AT-1-expressing COS-7 cells after metabolic labeling with [^{14}C]palmitic acid (31). However, it remained to be solved whether PLA/AT proteins actually function as *N*-acyltransferases *in vivo*. Here, we show by metabolic labeling with [^{14}C]ethanolamine and liquid chromatography-tandem mass spectrometry (LC-MS/MS) that the expression of PLA/AT family proteins in animal cells significantly increases intracellular levels of NAPE and NAE. We also show that additional introduction of *NAPE-PLD* into PLA/AT-2-expressing cells enhances intracellular conversion of accumulating NAPE to NAE. These results suggest that PLA/AT proteins may function as NAPE-forming *N*-acyltransferases in living cells.

EXPERIMENTAL PROCEDURES

Materials—[1-^{14}C]Palmitic acid and 1,2-[1-^{14}C]dipalmitoylphosphatidylcholine (PC) were purchased from PerkinElmer Life Sciences. [1,2-^{14}C]Ethanolamine-HCl ([^{14}C]ethanolamine) was from Moravek Biochemicals (Brea, CA). 1-Palmitoyl-2-[1-^{14}C]palmitoyl-PC, horseradish peroxidase-linked anti-mouse IgG, horseradish peroxidase-linked anti-rabbit IgG, Hybond P, and an ECL Plus kit were from GE Healthcare. 1,2-Dipalmitoyl-PC, 1,2-dipalmitoyl-PE, 1,2-dioleoyl-PE, and monoclonal antibody against 70-kDa peroxisomal membrane protein (PMP70), anti-FLAG M2 antibody, A23187, and forskolin were from Sigma. 1-*O*-1′(*Z*)-Octadecenyl-2-oleoyl-glycerophosphoethanolamine and 1,2-dimyristoyl-PE were from Avanti Polar Lipids (Alabaster, AL). Heptadecanoic acid was from Doosan Serdary Research Laboratories (Toronto, Ontario, Canada). Dulbecco's modified Eagle's medium, Lipofectamine 2000, Lipofectamine RNAiMAX, and small interfering RNAs (siRNAs) directed against human PLA/AT-2 (siPLA/AT-2-1, HRASLS2-HSS123656; siPLA/AT-2-2, HRASLS2-HSS123657), a control siRNA, fetal calf serum, geneticin, and pEF1/Myc-His vector were from Invitrogen. URB597, *N*-palmitoylethanolamine, and *N*-(2-hydroxyethyl)-hexadecanamide 7,7,8,8-d_4 (deuterated *N*-palmitoylethanolamine) were from Cayman Chemical (Ann Arbor, MI). Nonidet P-40 and Triton X-100 were from Nacalai Tesque, Inc. (Kyoto, Japan). *Ex* Taq DNA polymerase and a PrimeScript RT reagent kit were from TaKaRa Bio Inc. (Ohtsu, Japan). The RNeasy mini kit was from Qiagen. KOD-Plus DNA polymerase was from TOYOBO (Osaka, Japan). The anti-catalase antibody was from Abcam Inc. (Cambridge, MA). Protein assay dye reagent concentrate was from Bio-Rad. Phorbol 12-myristate 13-acetate (PMA) and precoated Silica Gel 60 F_{254} aluminum sheets (20 × 20 cm, 0.2-mm thick) for thin layer chromatography (TLC) were from Merck. *N*-[^{14}C]Palmitoyl-PE was prepared from [1-^{14}C]palmitic acid and 1,2-dioleoyl-PE according to the method of Schmid *et al.* (32). *N*-Heptadecanoyl-1,2-dipalmitoyl-PE and *N*-heptadecanoyl-1-*O*-1′(*Z*)-octadecenyl-2-oleoyl-glycerophosphoethanolamine were also prepared with 1.5 mol eq of heptadecanoic acid and *N*,*N*′-dicyclohexylcarbodiimide as described (32), and purified by TLC on a silica gel plate developed with a solvent system of chloroform, methanol, 28% ammonium hydroxide (80:20:2, v/v). 1-[1-^{14}C]Palmitoyl-2-palmitoyl-PC was prepared from 2-palmitoyl-glycerophosphocholine and [1-^{14}C]palmitic acid (16). *N*-[^{14}C]Palmitoylethanolamine was prepared from [^{14}C]palmitic acid and ethanolamine (33). *N*-[^{14}C]Palmitoyl-lyso-PE was prepared as described previously (18). *sn*-Glycero-3-phospho-*N*-heptadecanoylethanolamine was prepared by alkaline hydrolysis of 5 μmol of *N*-heptadecanoyl-1,2-dipalmitoyl-PE with 0.1 N KOH in methanol at 60 °C for 10 min. The reaction product was extracted from the neutralized reaction mixture by the method of Bligh and Dyer (34) and purified by TLC developed with chloroform, methanol, 20% ammonium hydroxide (65:35:8, v/v).

Construction of Expression Vectors—The cDNAs encoding N-terminally FLAG-tagged PLA/AT-1–5 were amplified by PCR. The templates used were cDNAs of human PLA/AT-1–5 cloned previously (28, 30, 31). The following SpeI site-containing oligonucleotides and NotI site-containing oligonucleotides were used as forward and reverse primers, respectively: PLA/AT-1, 5′-CGCACTAGTGGAAAATGGATTACAAGGATGACGACGATAAGGCGTTTAATGATTGCTTCAGTTTG-3′ and 5′-CGCGCGGCCGCTTAATAGTATTTTGCTCTTTGTCCTT-3′; PLA/AT-2, 5′-CGCACTAGTGGAAAATGGATTACAAGGATGACGACGATAAGGCTTTGGCCAGACCAAGACCGAGA-3′ (primer A) and 5′-CGCGCGGCCGCTTATTGCCTTTCCCGCTTGCTTCTGG-3′ (primer B); PLA/AT-3, 5′-CGCACTAGTGGAAAATGGATTACAAGGATGACGACGATAAGCGTGCGCCCATTCCAGAGCCTAAG-3′ and 5′-CGCGCGGCCGCTTATTGCTTTTGTCGCTTGTTTC-3′; PLA/AT-4, 5′-CGCACTAGTGGAAAATGGATTACAAGGATGACGACGATAAGGCTTCGCCACACCAAGAGCCCAAA-3′ and 5′-CGCGCGGCCGCTCAGGCTGTCGCTTTTTTTGGTATC-3′; and PLA/AT-5, 5′-CGCACTAGTGGAAAATGGATTACAAGGATGACGACGATAAGGGCCTGAGCCCGGGCGCC-3′ and 5′-CGCGCGGCCGCTCAGGCAGTTATTGGTTTGG-3′. PCR was carried out with KOD-Plus DNA polymerase for 30 cycles at 94 °C for 20 s, 56 °C for 20 s, and 68 °C for 60 s in 5% (v/v) Me_2SO. Obtained DNA fragments were subcloned into SpeI and NotI sites of the pEF1/Myc-His vector. The cDNA encoding C113S mutant of PLA/AT-2 was prepared by megaprimer PCR, consisting of two sets of PCRs, using pEF1/Myc-His vector harboring PLA/AT-2 as a template. An oligonucleotide 5′-CTGACCAGTGACAACAGCGAGCACTTCGTG-3′ (the underline indicates the mismatch) and its complementary oligonucleotide were used as primers. Primers A and B were used as the forward primer and reverse primer, respectively. All constructs were sequenced in both directions using an ABI 3130 Genetic Analyzer (Invitrogen). The expression vectors pIREShyg2, harboring mouse NAPE-PLD (35), and pcDNA3.1(+), harboring human NAAA (22), were constructed as reported previously.

Expression of PLA/AT Family Members in Animal Cells—COS-7 cells were grown at 37 °C to 90% confluency in 100-mm dishes containing Dulbecco's modified Eagle's medium with 10% fetal bovine serum in a humidified 5% CO_2 and 95% air incubator. The expression vectors harboring N-terminally FLAG-tagged *PLA/AT-1–5* or the insert-free pEF1/Myc-His vector were introduced into COS-7 cells using Lipofectamine 2000 according to the manufacturer's instructions. Forty eight hours after transfection, cells were harvested, sonicated three times each for 3 s in 20 mM Tris-HCl (pH 7.4), and used for

enzyme assays. For the experiments shown in Fig. 4, recombinant FLAG-tagged PLA/AT-2 was purified by anti-FLAG M2 affinity chromatography as described previously (30). For the stable expression of PLA/AT-2, HEK293 cells were transfected with pEF1/Myc-His vector harboring N-terminally FLAG-tagged *PLA/AT-2* or the insert-free pEF1/Myc-His vector using Lipofectamine 2000. Cells were selected in the medium containing 1 mg/ml geneticin. Clonal cell lines PLA/AT-2-H and PLA/AT-2-L were isolated by colony lifting, and propagated. PLA/AT-3-expressing HEK293 cells were established previously (36).

Enzyme Assays—For the *N*-acyltransferase assay, cell homogenates (30 μg of protein) were incubated with 40 μM 1,2-[1-^{14}C]dipalmitoyl-PC (45,000 cpm) and 75 μM 1,2-dioleoyl-PE in 100 μl of 50 mM glycine-NaOH (pH 9.0), 2 mM dithiothreitol (DTT), 1 mM EDTA, and 0.1% Nonidet P-40 at 37 °C for 30 min. For the NAPE-PLD assay, cell homogenates (30 μg of protein) were incubated with 100 μM *N*-[^{14}C]palmitoyl-PE (10,000 cpm) in 100 μl of 50 mM Tris-HCl (pH 7.4), 1 mM $MgCl_2$, and 0.1% Triton X-100 at 37 °C for 10 min. For the NAAA assay, cell homogenates (30 μg of protein) were incubated with 200 μM *N*-[^{14}C]palmitoylethanolamine (20,000 cpm, dissolved in 10 μl of Me_2SO) in 100 μl of 100 mM citrate-sodium phosphate (pH 4.5), 3 mM DTT, 0.1% Nonidet P-40, 0.05% bovine serum albumin, and 150 mM NaCl at 37 °C for 30 min. Reactions were terminated by the addition of 320 μl of a mixture of chloroform/methanol (2:1, v/v) containing 5 mM 3(2)-*t*-butyl-4-hydroxyanisole (for *N*-acyltransferase and NAPE-PLD assays) or a mixture of diethyl ether, methanol, and 1 M citric acid (30:4:1, v/v) containing 5 mM 3(2)-*t*-butyl-4-hydroxyanisole (for the NAAA assay). After centrifugation, 100 μl of the organic phase was spotted on a silica gel thin layer plate (10-cm height) and developed at 4 °C for 25 min in chloroform, methanol, 28% ammonium hydroxide (80:20:2, v/v) (solvent A). The distribution of radioactivity on the plate was visualized and quantified using a BAS1500 bioimaging analyzer (FUJIX Ltd., Tokyo, Japan). Protein concentration was determined by the method of Bradford with bovine serum albumin as a standard.

RT-PCR—Total RNAs were isolated from cells using an RNeasy mini kit. cDNAs were prepared from 1 μg of total RNA using a PrimeScript RT reagent kit and subjected to PCR amplification by *Ex* TaqDNA polymerase. The forward and reverse primers used were as follows: human PLA/AT-2, 5′-GGCTATGCACACTGGGCCATCTACG-3′ and 5′-GTTGGTCAGGGCAGACAGGACACTG-3′ (nucleotides 117–141 and 203–227, respectively, in GenBank™ accession number NM_017878); human PMP70, 5′-GTCATTGTCGAAAGGTTGGCATCAC-3′ and 5′-AGTTGCCTCTGCCATCCATATGCAG-3′ (nucleotides 1934–1958 and 2011–2035 in NM_002858); human catalase, 5′-AAGGTTTGGCCTCACAAGGACTACCCTC-3′ and 5′-TAGGCAAAAAGGCGGCCCTGAAGCATTTTG-3′ (nucleotides 990–1017 and 1133–1162 in NM_001752); human GAPDH, 5′-CGCTGAGTACGTCGTGGAGTCCACT-3′ and 5′-AGCAGAGGGGGCAGAGATGATGACC-3′ (nucleotides 375–399 and 456–480 in NM_002046). The PCR conditions used were as follows: denaturation at 96 °C for 20 s, annealing at 60 °C for 20 s, and extension at 72 °C for 20 s (24 cycles for GAPDH and 28 cycles for PLA/AT-2, PMP70, and catalase). RT-PCR for PLA/AT-3 and PLA/AT-4 was performed as described previously (30). Semi-quantitative real time PCR analysis was performed with the aid of the ABI 3130 Genetic Analyzer (Invitrogen). The primers used were the same as those for conventional PCR, and the conditions were as follows: denaturation at 95 °C for 6 s, and annealing and extension at 62 °C for 20 s (40 cycles).

RNA Interference—siRNAs were introduced into PLA/AT-2-H cells or HeLa cells with Lipofectamine RNAiMAX according to the manufacturer's instructions. The final concentration of siRNA was 20 nM. Forty eight hours after transfection, cells were subjected to RT-PCR, the *N*-acyltransferase assay, metabolic labeling with [^{14}C]ethanolamine, or LC-MS/MS analysis.

Metabolic Labeling—Cells were grown at 37 °C to 80% confluency in a 100-mm dish containing Dulbecco's modified Eagle's medium with 10% fetal calf serum and were labeled with [^{14}C]ethanolamine (1.6 μCi) or [^{14}C]palmitic acid (1.6 μCi) for 18 h. Cells were then harvested and washed twice with PBS. Total lipids were extracted by the method of Bligh and Dyer (34), spotted on a silica gel thin layer plate (20-cm height), and developed at 4 °C for 90 min in solvent A. The distribution of radioactivity on the plate was visualized and quantified using a BAS1500 bioimaging analyzer.

Western Blotting—Cells were homogenized in homogenization buffer (0.25 M sucrose, 1 mM EDTA, and 20 mM HEPES (pH 7.4)) by being passed through a 27-gauge syringe (37, 38), and nuclei and unbroken cells were removed by centrifugation at 800 × *g* for 10 min at 4 °C. Postnuclear supernatant fractions were then centrifuged at 105,000 × *g* for 30 min at 4 °C to separate the cytosol (supernatant fractions) from cellular organelles (particulate fractions). Samples were separated by SDS-PAGE and electrotransferred to a hydrophobic polyvinylidene difluoride membrane (Hybond P). The membrane was blocked with PBS containing 5% dried milk and 0.1% Tween 20 (buffer A) and then incubated with primary antibodies (1:2000 dilution) in buffer A at room temperature for 1 h, followed by incubation with horseradish peroxidase-labeled secondary antibodies (1:4000 dilution) in buffer A at room temperature for 1 h. Proteins were finally treated with an ECL Plus kit and visualized with the aid of a LAS1000plus lumino-imaging analyzer (FUJIX Ltd.).

Lipid Analysis by LC-MS/MS—Lipids were extracted from cells by a modification of the method of Bligh and Dyer, essentially as described previously (39). In this method, cells were suspended in 3.8 ml of a mixture of chloroform, methanol, 0.07 M KCl (1:2:0.8, v/v) on ice followed by sonication for 10–20 s. A mixture of internal standards for LC-MS/MS was added to this suspension. After standing for 20 min on ice, the mixture was centrifuged at 1400 × *g* for 10 min. The supernatant was withdrawn, and the resultant pellet was mixed with 1.9 ml of chloroform/methanol/water (1:2:0.8) followed by centrifugation. Supernatants were combined, and 1.5 ml each of chloroform and water was added to the sample to produce phase separation. After centrifugation of the mixture, the organic lower phase was withdrawn. The upper layer was mixed with 3 ml of chloroform/methanol (17:3), and the mixture was centrifuged. Combined lower layers were evaporated to dryness under a stream of nitrogen gas, and half of this lipid extract was recon-

stituted in 0.1 ml of methanol/water (95:5, v/v) containing 0.05 M ammonium formate in an insert of a brown glass vial for LC-MS/MS. The lipid/phosphate concentration in another half of the lipid extract was determined as described previously (40).

LC-MS/MS was performed on a quadrupole-linear ion trap hybrid MS, 4000 Q TRAP (Applied Biosystems/MDS Sciex, Concord, Ontario, Canada) with a 1100 LC system (Agilent Technologies, Wilmington, DE) combined with an HTS-PAL autosampler (CTC Analytics AG, Zwingen, Switzerland), essentially as described previously (20). The extract was analyzed for molecular species of NAPE by LC on an Imtakt Unison UK-Amino column (100 × 2 mm, 3.0-μm particle size) at a flow rate of 0.1 ml/min. The mobile phase was a mixture of acetonitrile/methanol (95:5, v/v) containing 0.1% triethylamine. The molecular species of glycerophospho-*N*-acylethanolamine (GP-NAE) and NAE in the extract were separated on a Supelco Ascentis Express C18 reverse phase column (100 × 2.1 mm, 2.7-μm particle size) with methanol/water (95:5) containing 5 mM ammonium formate at a flow rate of 0.20 (for GP-NAE) or 0.15 ml/min (for NAE). The molecular species of PE were separated by LC on Cadenza CD-C18 (100 × 1.0 mm, 3-μm particle) with acetonitrile/methanol (1:1) containing 5 mM ammonium formate at a flow rate of 0.15 ml/min. Routinely, 5-μl aliquots of the test solution in an insert were applied using the autosampler. In the negative ion mode of operation with multiple reaction monitoring, $[R_2COO]^-$ and the deprotonated molecular ion for NAPE were selected for Q3 and Q1. In the positive ion mode of operation with multiple reaction monitoring, $[\text{ethanolamine}]^+$ at *m/z* 62 for NAE and $[M + H - \text{phosphoethanolamine}]^+$ for PE were selected as Q3 in combination with the protonated molecular ion as Q1. The molecular species of NAE, NAPE, and diacyl-PE were quantified using deuterated *N*-palmitoylethanolamine, *N*-heptadecanoyl-1,2-dipalmitoyl-PE, and 1,2-dimyristoyl-PE as internal standards, respectively. Corrections were made for the quantification of molecular species of *N*-acylated plasmenylethanolamine (pNAPE) and plasmenylethanolamine based on the slopes of the calibration lines constructed with *N*-heptadecanoyl-1-*O*-1′(*Z*)-octadecenyl-2-oleoyl-glycerophosphoethanolamine (external standard) *versus* *N*-heptadecanoyl-1,2-dipalmitoyl-PE (internal standard for *N*-acyl-PE) and 1-*O*-1′(*Z*)-octadecenyl-2-oleoyl-glycerophosphoethanolamine (external standard) *versus* 1,2-dimyristoyl-PE (internal standard for PE), respectively. Negative ions due to the molecular species of GP-NAE were quantified at a combination of deprotonated molecular ions and $[\text{glycerophosphate (171)}]^-$ for Q1 and Q3, based on the peak ratios relative to glycerophospho-*N*-heptadecanoylethanolamine. Values are represented as picomoles/μmol or nanomoles/μmol of total phospholipids.

RESULTS

Generation of NAPE in Cells Overexpressing PLA/AT Family Members—To examine whether PLA/AT family members can generate NAPE in living cells, we transiently expressed each of the PLA/AT-1–5 in COS-7 cells. Expression was confirmed by Western blotting with an anti-FLAG antibody, which recognized the FLAG tag attached to recombinant PLA/AT-1–5 (data not shown). Homogenates of the transfectants were allowed to react with 1,2-[^{14}C]dipalmitoyl-PC and dioleoyl-PE as an acyl donor and an acyl acceptor in the *N*-acyltransferase reaction, respectively, and products were separated by TLC. The results showed the formation of a radioactive band corresponding to *N*-palmitoyl-PE by all of PLA/AT-1–5 (Fig. 2*A*). A radioactive band corresponding to free palmitic acid was also detected in each PLA/AT as the $PLA_{1/2}$ reaction product. The ratio of *N*-acyltransferase activity to $PLA_{1/2}$ activity was largely different among PLA/AT-1–5 (Fig. 2*B*). The highest ratio (5.6) was seen with PLA/AT-2, followed by PLA/AT-5 and -1. Conversely, PLA/AT-3 and -4 showed lower ratios (<1). A radioactive band comigrated with authentic *N*-palmitoyl-lyso-PE also being detected. On the other hand, *N*-palmitoyl-PE and *N*-palmitoyl-lyso PE were hardly detectable with the homogenate of COS-7 cells transfected with the insert-free vector.

Next, these cells were metabolically radiolabeled with [^{14}C]ethanolamine, and total lipids extracted from cells were analyzed by TLC. As shown in Fig. 2*C*, radioactive bands that comigrated with authentic *N*-palmitoyl-PE, *N*-palmitoylethanolamine, and *N*-palmitoyl-lyso-PE were clearly detected in most PLA/AT-expressing cells. The radioactive substance corresponding to NAPE was extracted from the silica gel plate and treated with recombinant NAPE-PLD, an enzyme that specifically hydrolyzes NAPE to NAE and phosphatidic acid. This treatment led to the production of a radioactive band that comigrated with authentic *N*-palmitoylethanolamine (Fig. 2*F*), confirming that the original band is NAPE. When radioactive NAPE was quantified (Fig. 2*D*), high levels of NAPE (19.4 and 8.9% of total radioactivity) were detected in PLA/AT-2-expressing cells and PLA/AT-1-expressing cells, respectively, followed by PLA/AT-4-expressing cells and PLA/AT-5-expressing cells. Although PLA/AT-3 cells generated a small amount of NAPE, its level was not significantly different from that in control COS-7 cells. The content of NAE also showed a similar tendency with the highest level (1.6% of total radioactivity) in PLA/AT-2 cells (Fig. 2*E*). We also labeled these cells with [^{14}C]palmitic acid and confirmed the generation of [^{14}C]NAPE in cells expressing PLA/AT-1, -2, -4, or -5, with the highest NAPE radioactivity in PLA/AT-2 cells (Fig. 2*G*). These results showed that PLA/AT-1, -2, -4, and -5 have the capability to generate NAPE in living cells. Because PLA/AT-2-expressing cells showed the highest levels of NAPE and NAE, we focused on the characterization of PLA/AT-2 hereafter.

NAPE Formation by PLA/AT-2 Requires Its Enzyme Activity—Because Cys-113 of PLA/AT-2 is presumed to be a catalytic nucleophile (30), its C113S mutant was expected to be catalytically inactive. We thus constructed this mutant, transiently expressed it in COS-7 cells, and confirmed its expression by Western blotting (Fig. 3*A*). The cell homogenate was essentially free of *N*-acyltransferase (Fig. 3*B*), and metabolic labeling of C113S-expressing cells with [^{14}C]ethanolamine did not increase levels of radioactive NAPE (Fig. 3*C*) and NAE (Fig. 3*D*). These results strongly suggest that the enzyme activity of PLA/AT-2 is required for the production of NAPE and NAE in PLA/AT-2-expressing cells.

PLA/AT-2 Preferentially Transfers sn-1 Acyl Chain of Phospholipid to PE—We earlier found that the purified recombinant PLA/AT-2, which functions as a $PLA_{1/2}$ enzyme, preferentially

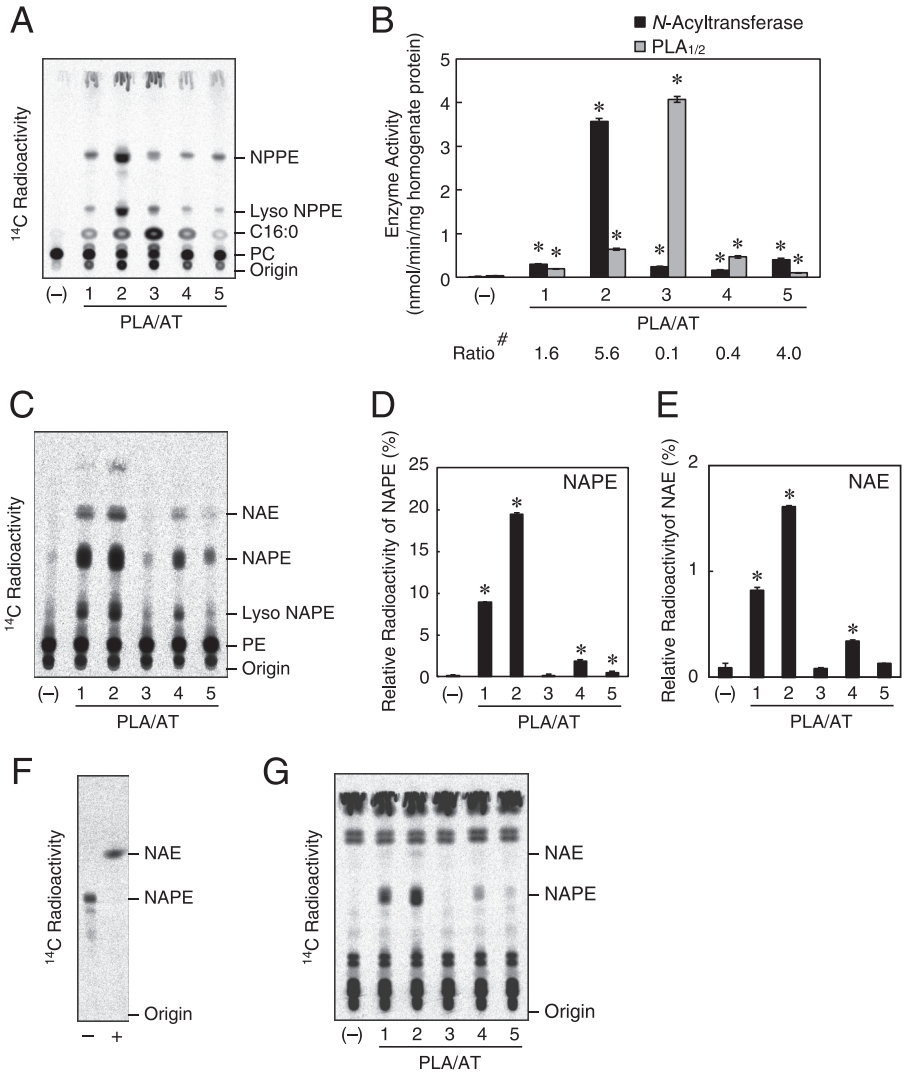

FIGURE 2. **Production of NAPE and NAE in COS-7 cells transiently expressing PLA/AT family members.** COS-7 cells were transiently transfected with the insert-free vector (*lanes* (−)) or expression vectors harboring human *PLA/AT-1–5* (*lanes 1–5*, respectively). Homogenates (30 μg of protein) of cells were incubated with 40 μM 1,2-[1-^{14}C]dipalmitoyl-PC and 75 μM 1,2-dioleoyl-PE, and the resultant products were separated by TLC (*A*). In this assay, *N*-palmitoyl-PE-forming activity and free palmitic acid-forming activity were regarded as *N*-acyltransferase activity and $PLA_{1/2}$ activity, respectively, and these activities were quantified (mean values ± S.D. (*error bars*), $n = 3$) (*B*). #, ratio of *N*-acyltransferase activity to $PLA_{1/2}$ activity in each PLA/AT is shown (*B*). *C*–*E*, living cells were incubated with [^{14}C]ethanolamine, and their total lipids were extracted. Radiolabeled lipids were then separated by TLC (*C*). Relative radioactivities of NAPE (*D*) and NAE (*E*) are shown (mean values ± S.D. (*error bars*), $n = 3$). The radioactive substance corresponding to NAPE was extracted from the band on the TLC plate and treated with recombinant NAPE-PLD (*lane* +) or buffer alone (*lane* −) (*F*). Cells were radiolabeled with [^{14}C]palmitic acid, and their total lipids were separated by TLC (*G*). *Asterisks* indicate significant differences from control cells ($p < 0.005$). *A*, *C*, *F*, and *G*, the positions of authentic compounds on the TLC plate are indicated. *NPPE*, *N*-palmitoyl-PE; *lyso-NPPE*, *N*-palmitoyl-lyso-PE; *C16:0*, palmitic acid.

releases *sn*-1 fatty acid over *sn*-2 fatty acid from glycerophospholipids (30). To determine which acyl chain is utilized in the *N*-acyltransferase reaction, we allowed the purified PLA/AT-2 to react with 1-[^{14}C]palmitoyl-2-palmitoyl-PC, 1-palmitoyl-2-[^{14}C]palmitoyl-PC, or 1,2-[^{14}C]dipalmitoyl-PC as acyl donors in the presence of nonradiolabeled PE as an acyl acceptor. As shown in Fig. 4, *N*-[^{14}C]palmitoyl-PE-forming activity with 1-[^{14}C]palmitoyl-2-palmitoyl-PC (37.0 nmol/min/mg of protein) was much higher than that with 1-palmitoyl-2-[^{14}C]palmitoyl-PC (2.5 nmol/min/mg of protein). In accordance with this result, a much higher amount of [^{14}C]lyso-PC, another product of *N*-acyltransferase, was formed from 1-palmitoyl-2-[^{14}C]palmitoyl-PC than from 1-[^{14}C]palmitoyl-2-palmitoyl-PC (Fig. 4*A*). These results indicated that PLA/AT-2 preferentially transfers an acyl chain from the *sn*-1 position of glycerophospholipid to the amino group of PE.

Constitutive Expression of PLA/AT-2 in HEK293 Cells Leads to the Accumulation of NAPE—We established two HEK293 cell lines that stably express PLA/AT-2 under the control of human elongation factor 1α-subunit promoter (PLA/AT-2-H and PLA/AT-2-L cells). As analyzed by semiquantitative real time PCR, the expression level of PLA/AT-2 mRNA in PLA/AT-2-H cells was about 2-fold higher than that in PLA/AT-2-L cells (Fig. 5*A*). mRNA of PLA/AT-2 was negligible in HEK293 cells transfected with the insert-free vector. *N*-Acyltransferase activity in the homogenate of PLA/AT-2-H cells was about 2-fold higher than that of PLA/AT-2-L cells (Fig. 5, *B* and *C*). When 1 mM EDTA was replaced with 1 mM Ca^{2+}, activity did

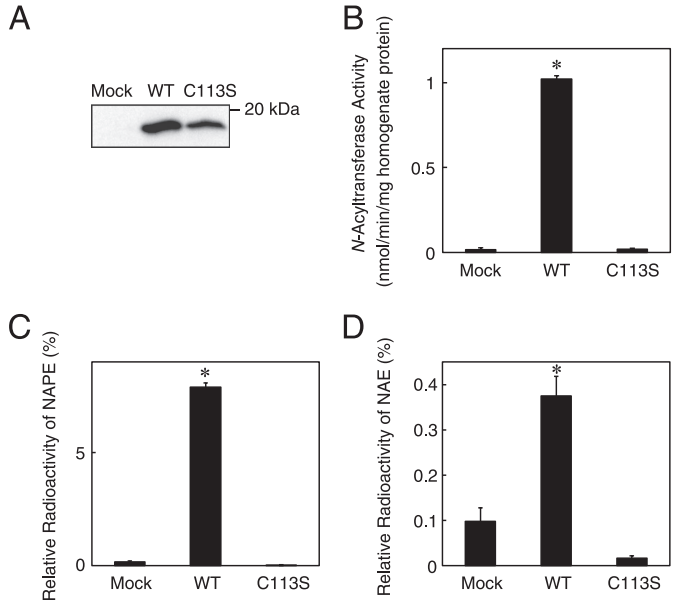

FIGURE 3. **Enzyme activity of PLA/AT-2 is required for the production of NAPE.** COS-7 cells were transiently transfected with the insert-free vector, expression vector harboring human wild-type *PLA/AT-2* (*WT*), or its mutant *C113S*. Homogenates (30 μg of protein) of cells were subjected to Western blotting with the anti-FLAG antibody (*A*) and the *N*-acyltransferase assay (*B*) as described under "Experimental Procedures." *B*, enzyme activities were quantified (mean values ± S.D. (*error bars*), $n = 3$). For metabolic radiolabeling experiments, cells were incubated with [^{14}C]ethanolamine, and their total lipids were analyzed by TLC. Relative radioactivities of NAPE (*C*) and NAE (*D*) are shown (mean values ± S.D. (*error bars*), $n = 3$). *Asterisks* indicate significant differences from control cells ($p < 0.01$).

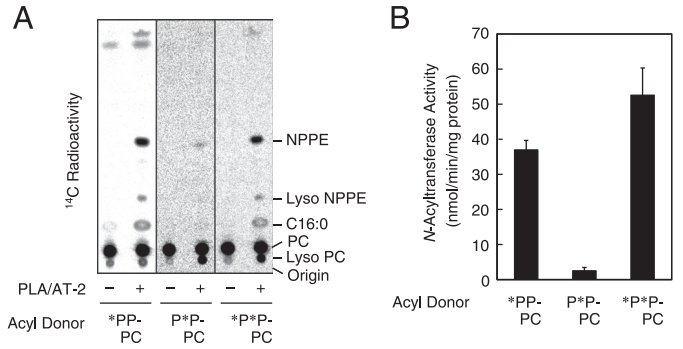

FIGURE 4. **Reactivities of purified PLA/AT-2 with region-specific radiolabeled PCs.** Purified recombinant human PLA/AT-2 (0.15 μg of protein) (*lanes* +) or buffer alone (*lanes* −) was allowed to react with 40 μM of 1-[^{14}C]palmitoyl-2-palmitoyl-PC (*PP-PC), 1-palmitoyl-2-[^{14}C]palmitoyl-PC (P*P-PC), or 1,2-[^{14}C]dipalmitoyl-PC (*P*P-PC) in the presence of 75 μM of 1,2-dioleoyl-PE. Products were separated by TLC (*A*) and *N*-acyltransferase activity was quantified (mean values ± S.D. (*error bars*), $n = 3$) (*B*). The positions of authentic compounds on the TLC plate are indicated. *NPPE*, *N*-palmitoyl-PE; *lyso-NPPE*, *N*-palmitoyl-lyso-PE; *C16:0*, palmitic acid.

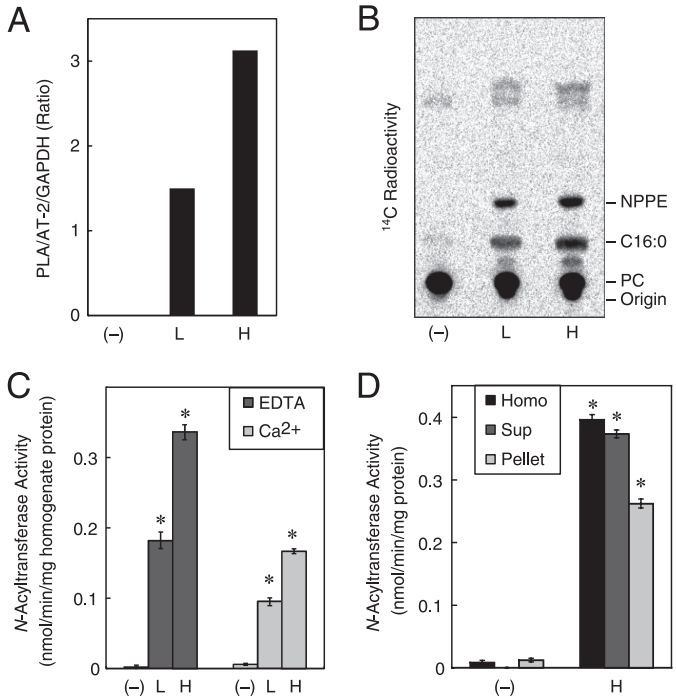

FIGURE 5. **Stable expression of PLA/AT-2 in HEK293 cells.** The expression of PLA/AT-2 mRNA was analyzed by semiquantitative real time PCR (*A*). GAPDH was used as a control. −, mock-transfected HEK293 cells; *L*, PLA/AT-2-L cells; *H*, PLA/AT-2-H cells. Cell homogenates (30 μg of protein) were assayed for *N*-acyltransferase activity as described under "Experimental Procedures," and products were separated by TLC (*B*). The positions of authentic compounds on the TLC plate are indicated. *NPPE*, *N*-palmitoyl-PE; *C16:0*, palmitic acid. The *N*-acyltransferase assay was performed in the presence of 1 mM EDTA or 1 mM $CaCl_2$ (*C*). Cell homogenates (*Homo*), soluble fractions (*Sup*), and particulate fractions (*Pellet*) (30 μg of protein) were also assayed (*D*). Enzyme activity is shown as mean values ± S.D. (*error bars*, $n = 3$) (*C* and *D*). *Asterisks* indicate significant differences from control cells ($p < 0.001$).

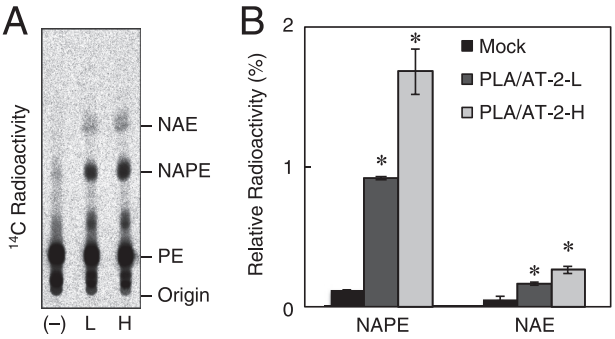

FIGURE 6. **Metabolic labeling of PLA/AT-2-expressing cells with [^{14}C]ethanolamine.** Cells were radiolabeled with [^{14}C]ethanolamine, and their total lipids were separated by TLC (*A*). The positions of authentic compounds on the TLC plate are indicated. −, mock-transfected HEK293 cells; *L*, PLA/AT-2-L cells; *H*, PLA/AT-2-H cells. Relative radioactivities of NAPE and NAE are shown (mean values ± S.D. (*error bars*), $n = 3$) (*B*). *Asterisks* indicate significant differences from control cells ($p < 0.005$).

not increase but decreased by about 50% (Fig. 5*C*). When the homogenate of PLA/AT-2-H cells was centrifuged at 105,000 × *g*, both soluble and particulate fractions showed *N*-acyltransferase activity with a 1.4-fold higher activity in the soluble fraction (Fig. 5*D*).

To examine the intracellular generation of NAPE, PLA/AT-2-L and PLA/AT-2-H cells were metabolically radiolabeled with [^{14}C]ethanolamine. When total lipids were extracted from cells and separated by TLC, NAPE levels in these cells were 7.7- and 14.1-fold higher than that of control HEK293 cells, respectively (Fig. 6, *A* and *B*). NAE levels also increased 2.8- and 4.6-fold (Fig. 6*B*). Thus, cellular levels of NAPE and NAE in these two PLA/AT-2-expressing cells correlated well with PLA/AT-2 mRNA levels and *N*-acyltransferase activities in the homogenates.

To rule out the possibility that the accumulation of NAPE was caused by the insertion of the *PLA/AT-2* gene into a specific region of the genome that contains one or more genes related to the metabolism of NAPE, we suppressed the expression of recombinant PLA/AT-2 in PLA/AT-2-H cells by two

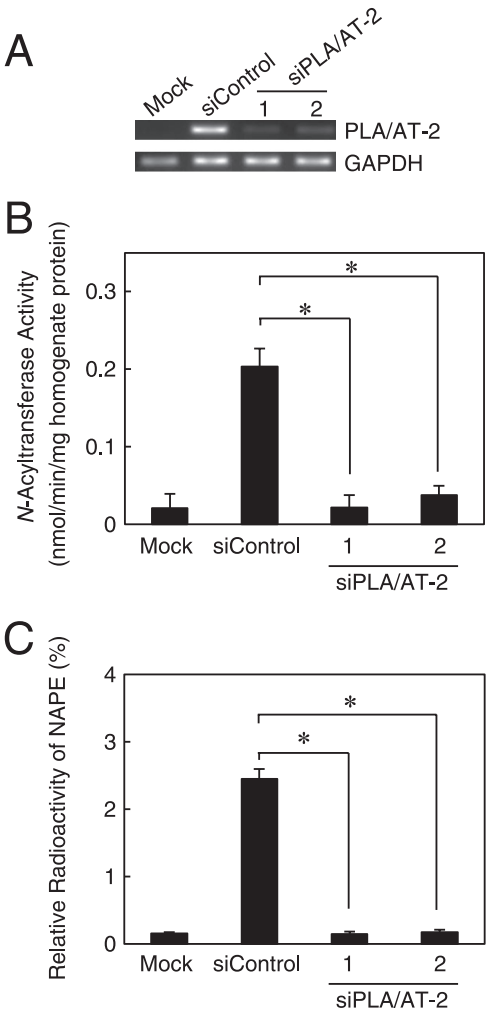

FIGURE 7. **Knockdown of PLA/AT-2 in PLA/AT-2-H cells.** PLA/AT-2-H cells were transfected with a control siRNA (*siControl*) or PLA/AT-2 siRNAs (*siPLA/AT-2–1 and -2*) (*A*). After 48 h, total RNAs were isolated and analyzed by RT-PCR using specific primers for the mRNAs of PLA/AT-2 and GAPDH (a control). Cell homogenates (30 μg of protein) were subjected to the *N*-acyltransferase assay as described under "Experimental Procedures" (*B*). Enzyme activity is shown as mean values ± S.D. (*error bars*, $n = 3$). Cells were radiolabeled with [^{14}C]ethanolamine, and their total lipids were separated by TLC (*C*). Relative radioactivities of NAPE are shown (mean values ± S.D. (*error bars*), $n = 3$). *Asterisks* indicate significant differences from siControl cells ($p < 0.005$).

siRNAs targeting different regions of *PLA/AT-2*. As shown in Fig. 7*A*, RT-PCR analysis revealed a strong suppression of *PLA/AT-2* mRNA expression in cells treated with PLA/AT-2 siRNAs. *N*-Acyltransferase activities in the homogenates of PLA/AT-2 knockdown cells were reduced to 11–19% that of cells treated with a control siRNA (Fig. 7*B*). When knockdown cells were labeled with [^{14}C]ethanolamine, NAPE levels almost completely reverted to that of control cells (Fig. 7*C*). These results confirmed that the stable expression of PLA/AT-2 causes the accumulation of NAPE in living HEK293 cells by its *N*-acyltransferase activity.

Analysis of NAPEs, pNAPEs, and Their Metabolites by LC-MS/MS—We next analyzed the molecular species of *N*-acylated ethanolamine phospholipids and their metabolites in PLA/AT-2-H cells and control HEK293 cells by LC-MS/MS. Concerning *N*-acylated ethanolamine phospholipids, we measured both the diacyl-type (NAPE) and plasmalogen-type (pNAPE) (Fig. 8). We confirmed the preferential liberation of the *sn*-2 fatty acyl group over the *sn*-1 fatty acyl group from a standard *N*-heptadecanoyl-PE (1-palmitoyl-2-oleoyl) under our conditions for tandem mass spectrometry. However, we could not exclude a possibility that $[R_1COO]^-$ was partially involved in the ion peaks assigned as $[R_2COO]^-$ when endogenous NAPE species were analyzed. Thus, we tentatively assigned the molecular species of NAPE (diacyl) in terms of both the combined chain length and unsaturation degree of the *sn*-1 *O*- and *N*-linked fatty acyl moieties together with those of *sn*-2 *O*-linked fatty acyl moiety. As shown in Fig. 8*A*, the expression of PLA/AT-2 remarkably increased endogenous levels of most species of NAPE. Major *sn*-1 *O*-acyl + *N*-acyl species of NAPE in PLA/AT-2-H cells were 32:0, 32:1, 34:0, 34:1, 36:0, 36:1, and 36:2. The total amount of NAPE species in cells was 13-fold larger than that in control cells. The *sn*-2 *O*-acyl chains of NAPE were mostly 18:1. However, the amounts of most pNAPE species were slightly increased or almost unaltered by the expression of PLA/AT-2 (Fig. 8*B*). The total amount of pNAPE species in PLA/AT-2-H cells was only 1.4-fold larger than that in control cells.

As shown in Fig. 9*A*, the major NAEs were 18:0, 16:0, and 18:1. The total amount of NAEs was 12-fold higher in PLA/AT-2 cells. A small amount of anandamide was detected only in PLA/AT-2-H cells. GP-NAE is an intermediate in the NAPE-PLD-independent pathway, which forms NAE from NAPE (20, 41). Various species of GP-NAE were remarkably increased by the overexpression of PLA/AT-2 (Fig. 9*B*). Major *N*-acyl species of GP-NAE were also 18:0, 16:0, and 18:1. These results showed that the expression of PLA/AT-2 causes remarkable increases in not only NAPEs but also their metabolites NAEs and GP-NAEs.

Peroxisomal Dysfunction of PLA/AT-2-H Cells—Our recent study revealed that the overexpression of PLA/AT-3 (H-rev107) results in a drastic decrease in the levels of ether-type lipids, including plasmenylethanolamine (36). We also found the dysfunction of peroxisomes, organelles involved in the biosynthesis of ether-type lipids, in PLA/AT-3-expressing cells. We therefore examined whether overexpression of PLA/AT-2 also decreases endogenous plasmenylethanolamine levels. As analyzed by LC-MS/MS (Fig. 10*B*), all species of plasmenylethanolamine were reduced in PLA/AT-2-H cells. The total amount of plasmenylethanolamine species was decreased by 91%. However, all species of diacyl-type PE were increased by the overexpression of PLA/AT-2 (Fig. 10*A*). Reductions in plasmenylethanolamine as a precursor of pNAPE may explain why pNAPE species were almost unaltered or slightly increased by the expression of PLA/AT-2 in contrast to the marked increase in NAPE species.

We also examined the expression and subcellular localization of PMP70 and catalase, two representative peroxisomal proteins, by Western blotting (Fig. 10*C*). In control cells, these proteins were localized in the particulate fraction as expected. However, in PLA/AT-2-H cells, PMP70 was hardly detected in the particulate or supernatant fraction, and catalase was detected mostly in the supernatant fraction. In contrast to their abnormal localization, RT-PCR analysis confirmed normal expression levels of PMP70 and catalase mRNAs in PLA/AT-

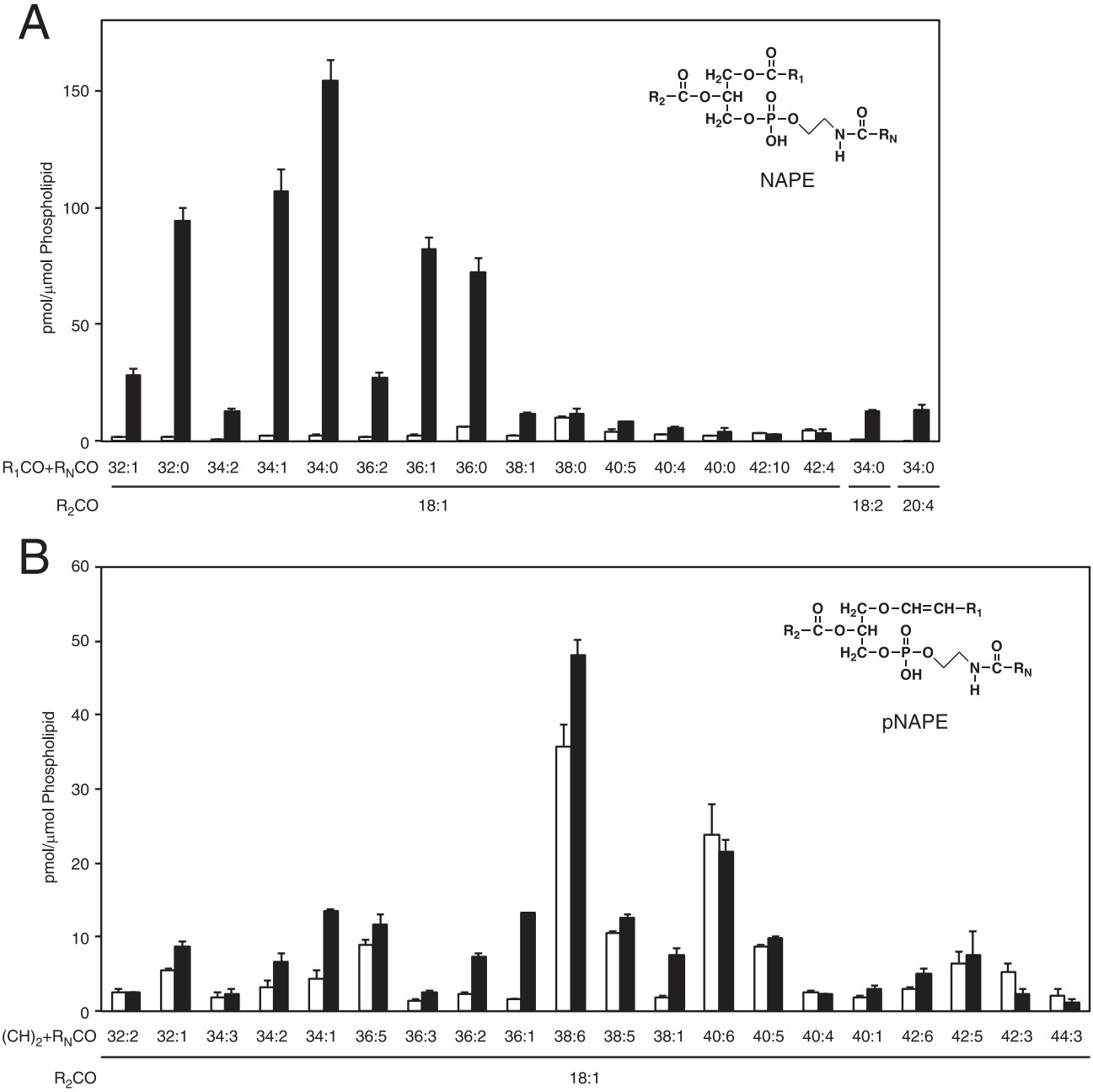

FIGURE 8. **LC-MS/MS analysis of *N*-acylated ethanolamine phospholipids in PLA/AT-2-H cells.** Various species of NAPEs (*A*) and pNAPEs (*B*) in PLA/AT-2-H cells (*closed columns*) and control cells (*open columns*) were analyzed by LC-MS/MS as described under "Experimental Procedures." *N*-Heptadecanoyl-1,2-dipalmitoyl-PE was used as an internal standard. pNAPEs levels were corrected based on the calibration line constructed with authentic *N*-heptadecanoyl-1-*O*-1′(*Z*)-octadecenyl-2-oleoyl-glycerophosphoethanolamine and *N*-heptadecanoyl-1,2-dipalmitoyl-PE (*B*). Results are shown as picomoles/μmol of total phospholipids (mean values ± S.D., $n = 2$). R_1CO+R_NCO and $R_1(CH)_2+R_NCO$ represent the total number of carbon atoms and double bonds in *sn*-1 *O*-acyl (or *sn*-1 *O*-alkenyl) and *N*-acyl chains.

2-H cells (Fig. 10*D*). Similar results were obtained with the peroxisomal proteins in PLA/AT-3-expressing cells (Fig. 10, *C* and *D*), in agreement with our previous report (36). These results strongly suggested that the expression of PLA/AT-2 as well as PLA/AT-3 causes the dysfunction of peroxisomes.

Expression of Related Enzymes in PLA/AT-2-expressing Cells—NAPE-PLD is a major enzyme responsible for the generation of NAE from NAPE. Overexpression of NAPE-PLD in mammalian cells leads to an increase in NAE levels with a concomitant decrease in NAPE levels (35). To examine whether the NAPE generated in PLA/AT-2-H cells can be metabolized by NAPE-PLD, we transiently expressed NAPE-PLD in PLA/AT-2-H cells. The homogenate of cells showed a NAPE-PLD activity as high as 27.1 nmol/min/mg protein, which produced *N*-palmitoylethanolamine from *N*-palmitoyl-PE (Fig. 11, *A* and *B*). Metabolic labeling with [^{14}C]ethanolamine revealed that the expression of NAPE-PLD results in a strong reduction in NAPE levels (Fig. 11, *C* and *D*). The concomitant increase in NAE levels was observed only in the presence of URB597, an FAAH inhibitor (Fig. 11, *C* and *D*) (42), suggesting rapid degradation of NAE by endogenous FAAH.

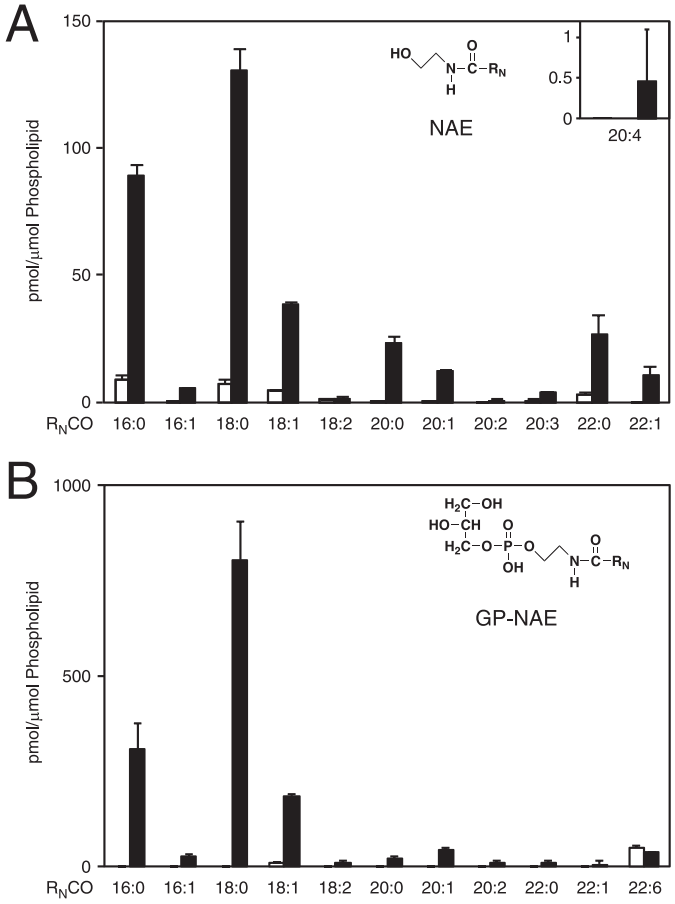

FIGURE 9. **LC-MS/MS analysis of NAEs and GP-NAEs in PLA/AT-2-H cells.** Various species of NAEs (*A*) and GP-NAEs (*B*) in PLA/AT-2-H cells (*closed columns*) and control cells (*open columns*) were analyzed by LC-MS/MS as described under "Experimental Procedures." NAE and GP-NAE species were quantified on the basis of peak ratios relative to deuterated *N*-palmitoylethanolamine and glycerophospho-*N*-heptadecanoylglycerol, respectively. Results are shown as picomoles/μmol of total phospholipids (mean values $\pm$ S.D., $n = 2$).

Next, we simultaneously expressed both NAPE-PLD and NAAA, an NAE-hydrolyzing enzyme different from FAAH (12), in PLA/AT-2-H cells. The transient expression of NAAA brought a high *N*-palmitoylethanolamine-hydrolyzing activity in the cell homogenate at pH 4.5, which is optimal for NAAA, whereas that of control cells expressing only NAPE-PLD was almost inactive under the same conditions (Fig. 12*A*). When cells were radiolabeled with [^{14}C]ethanolamine in the presence of URB597, NAE levels in NAAA-expressing cells decreased by 56% relative to control cells (Fig. 12, *B* and *C*). These results indicated that NAPE generated by PLA/AT-2 can be metabolized by NAPE-PLD and that the resultant NAE is degraded by FAAH and NAAA.

PLA/AT-2-dependent Formation of NAPE Is Not Enhanced by Cellular Stimuli—It was previously reported that Ca^{2+} ionophores A23187 and ionomycin increased NAPE levels in cortical neurons of rats and mice (14, 43). This Ca^{2+}-dependent formation of NAPE was attributed to Ca-NAT. Although NAPE formation by PLA/AT-2 was Ca^{2+}-independent (Fig. 5*C*), we were curious as to whether NAPE formation by PLA/AT-2 in living cells was stimulated by Ca^{2+} ionophores or other reagents. PLA/AT-2-H cells were labeled with [^{14}C]ethanolamine and then treated with A23187, forskolin (an adenylyl cyclase activator), or PMA (a protein kinase C activator) (Fig. 13). However, none of these reagents caused a significant increase in the levels of NAPE and NAE.

Possible Involvement of Endogenous PLA/AT-2 in NAPE Formation in HeLa Cells—HeLa cells endogenously express PLA/AT-2 (30). Therefore, we were interested in whether or not endogenous PLA/AT-2 was involved in NAPE formation in HeLa cells. We confirmed the expression of PLA/AT-2 mRNA by RT-PCR (Fig. 14*A*). mRNAs of PLA/AT-3 and -4 were also detected (Fig. 14*A*), whereas PLA/AT-1 and -5 were not detectable (data not shown). Introduction of two different siRNA constructs against PLA/AT-2 expectedly caused a decrease in PLA/AT-2 mRNA levels without affecting PLA/AT-3 and -4 levels (Fig. 14*A*). Both of the siRNA constructs reduced cellular levels of several species of NAPEs (Fig. 14*B*) and pNAPEs (Fig. 14*C*) in a similar manner. These results suggest that endogenous PLA/AT-2 is partly responsible for NAPE and pNAPE formation in HeLa cells.

DISCUSSION

NAPE is a class of endogenous glycerophospholipids and is well known to be precursors of bioactive NAEs (1, 2). The major route for NAPE formation in animal tissues is *N*-acylation of PE using glycerophospholipid as an acyl donor (13). The responsible enzyme Ca-NAT, however, remains molecularly uncharacterized. In contrast, we found an enzyme catalyzing the same reaction in a Ca^{2+}-independent manner, and we termed it Ca^{2+}-independent *N*-acyltransferase (iNAT, referred to as PLA/AT-5 in this study) (16, 28). Furthermore, we reported that other members of the PLA/AT family possess PE *N*-acyltransferase activity together with $PLA_{1/2}$ and lysophospholipid *O*-acyltransferase activities (30, 31). In humans, PLA/AT family members include A-C1 (PLA/AT-1), HRASLS2 (PLA/AT-2), H-rev107 (PLA/AT-3), tazarotene-induced protein 3 (TIG3, PLA/AT-4), and iNAT (PLA/AT-5). However, their roles in the *in vivo* formation of NAPE were poorly understood.

In this study, we first showed that transient expressions of PLA/AT-1, -2, -4, and -5 in COS-7 cells caused intracellular accumulation of NAPE. PLA/AT-3-expressing cells did not show a significant increase in NAPE levels, although the cell homogenate showed *N*-acyltransferase activity. The highest NAPE level in PLA/AT-2-expressing cells was consistent with the highest *N*-acyltransferase activity in their homogenate, and its enzymatically inactive mutant C113S failed to increase cellular NAPE levels. We have also reported that purified recombinant PLA/AT-2 showed the highest *N*-acyltransferase activity among purified PLA/AT family proteins (30, 31). We next revealed that endogenous levels of NAPE and NAE in HEK293 cells were markedly increased by stable expression of PLA/AT-2. With the aid of two clonal cells (PLA/AT-2-H and PLA/AT-2-L cells), which expressed PLA/AT-2 at different levels, we showed that expression levels of PLA/AT-2 correlated well with endogenous NAPE levels in living cells as well as *N*-acyltransferase activity in cell homogenates. Moreover, knockdown of overexpressed PLA/AT-2 by siRNAs largely reduced both *N*-acyltransferase activity and endogenous NAPE levels. These results confirmed that PLA/AT-2 functions as a NAPE-forming

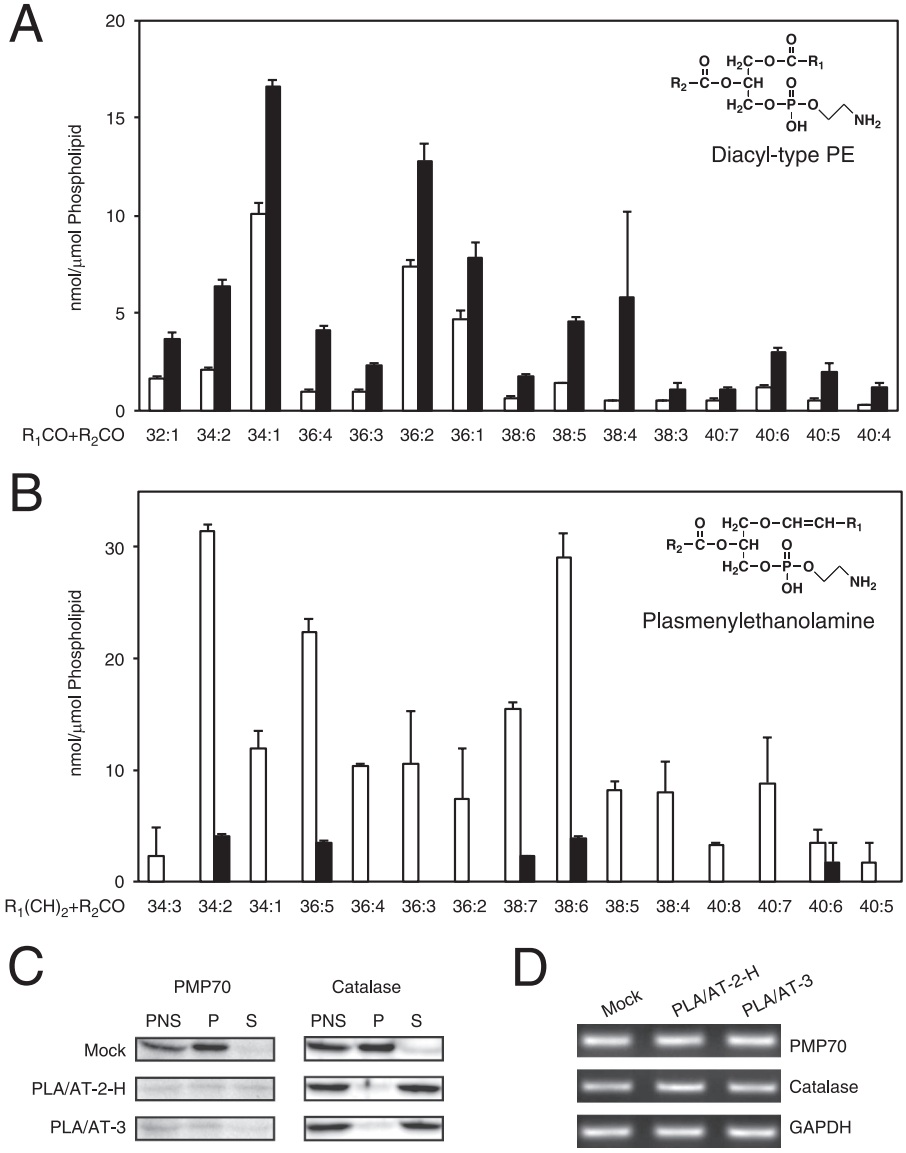

FIGURE 10. **LC-MS/MS analysis of PEs and plasmenylethanolamines and Western blot analysis of peroxisomal proteins in PLA/AT-2-H cells.** Various species of diacyl-type PEs (*A*) and plasmenylethanolamines (*B*) in PLA/AT-2-H cells (*closed columns*) and control cells (*open columns*) were analyzed by LC-MS/MS as described under "Experimental Procedures." 1,2-Dimyristoyl-PE was used as an internal standard. Plasmenylethanolamine levels were corrected based on the calibration line constructed with authentic dimyristoyl-PE and 1-*O*-1′(*Z*)-octadecenyl-2-oleoyl-glycerophosphoethanolamine (*B*). Results are shown as nanomoles/μmol of total phospholipids (mean values ± S.D., $n = 2$). *C*, postnuclear supernatant (*PNS*), particulate (*P*), and supernatant (*S*) fractions of control cells (*Mock*), PLA/AT-2-H cells (*PLA/AT-2-H*), and HEK293 cells overexpressing PLA/AT-3 (*PLA/AT-3*) were analyzed by Western blotting with antibodies against PMP70 and catalase. *D*, total RNAs were isolated from the indicated cells and were analyzed by RT-PCR using specific primers for PMP70, catalase, and GAPDH (a control).

N-acyltransferase in PLA/AT-2-expressing cells. Furthermore, the suppression of endogenous PLA/AT-2 in HeLa cells decreased the levels of several NAPE species. Taken together, our results suggest that members of the PLA/AT family may contribute at least partly to the generation of NAPE *in vivo*.

Although all PLA/AT members function as phospholipid-metabolizing enzymes, we should note that the ratio of *N*-acyltransferase activity to $PLA_{1/2}$ activity is different among members (Fig. 2*B*). The tissue distribution of each PLA/AT is also different (28–31). In addition, human tissues express all five members of the HRAS-like suppressor family (PLA/AT-1–5), although the genomes of rodents lack the genes of *PLA/AT-2* and *-4* (16, 28–31). These findings suggest that each PLA/AT plays different roles *in vivo*. Considering the lack of PLA/AT-2 in rodents, PLA/AT-1 and -5 may be responsible for NAPE formation in these animals. Especially, PLA/AT-1 is abundantly expressed in the testis, skeletal muscle, heart, and brain of rats and mice (31). Thus, it is of interest to examine whether this protein is involved in NAPE formation in these tissues.

PLA/AT-2-expressing cells generated a large amount of NAPE without any cellular stimuli. Addition of A23187, forskolin, or PMA to cells did not alter intracellular NAPE levels. This was consistent with the Ca^{2+} independency of *N*-acyltransferase activity in PLA/AT-2 (Fig. 5*C*). It is generally accepted that the formation of NAPE by *N*-acyltransferase is the principal rate-limiting step in the NAE-biosynthesizing pathway (13). In rat and mouse cortical neurons, Ca^{2+} ionophores augmented the generation of NAPE (14, 43), and this

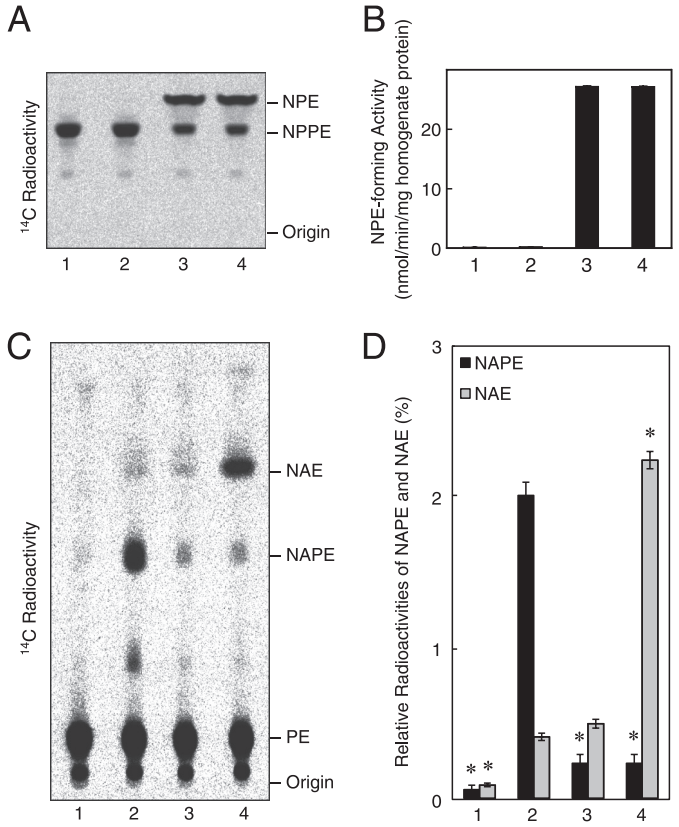

FIGURE 11. **Effect of NAPE-PLD expression on PLA/AT-2-H cells.** PLA/AT-2-H cells were transfected with the insert-free vector (*lane 2*) or expression vector harboring mouse *NAPE-PLD* (*lanes 3* and *4*) and incubated in the absence (*lanes 1–3*) or presence (*lane 4*) of 0.2 μM URB597 as described under "Experimental Procedures" (*A*). Control HEK293 cells transfected only with the insert-free vector were also analyzed (*lane 1*). Homogenates (30 μg of protein) of cells were subjected to the NAPE-PLD assay with 100 μM *N*-[^{14}C]palmitoyl-PE as substrate, and the resultant *N*-[^{14}C]palmitoylethanolamine was separated by TLC (*A*). *N*-Palmitoylethanolamine-forming activity was quantified (mean values ± S.D. (*error bars*), $n = 3$) (*B*). For metabolic radiolabeling experiments, cells incubated with [^{14}C]ethanolamine in the absence (*lanes 1–3*) or presence (*lane 4*) of 0.2 μM URB597, and their total lipids were separated by TLC (*C*). The relative radioactivities of NAPE and NAE are shown (mean values ± S.D. (*error bars*), $n = 3$) (*D*). *Asterisks* indicate significant differences from PLA/AT-2-H cells transfected with insert-free vector ($p < 0.002$). *A* and *C*, the positions of authentic compounds on the TLC plate are indicated. *NPPE*, *N*-palmitoyl-PE; *NPE*, *N*-palmitoylethanolamine.

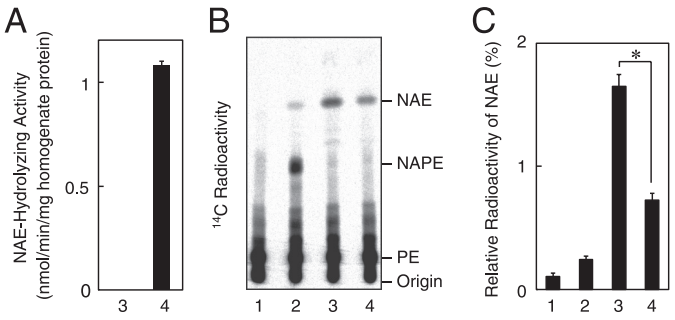

FIGURE 12. **Cotransfection of PLA/AT-2-H cells with NAPE-PLD and NAAA.** Control HEK293 cells (*lane 1*), PLA/AT-2-H cells (*lane 2*), PLA/AT-2-H cells transiently expressing mouse NAPE-PLD (*lane 3*), and PLA/AT-2-H cells transiently expressing both mouse NAPE-PLD and human NAAA (*lane 4*) were subjected to the NAAA assay (*A*) or metabolic labeling with [^{14}C]ethanolamine (*B* and *C*). Cell homogenates (30 μg of protein) were allowed to react with *N*-palmitoylethanolamine as described under "Experimental Procedures," and NAE-hydrolyzing activity was quantified (mean values ± S.D. (*error bars*), $n = 3$) (*A*). Cells were radiolabeled with [^{14}C]ethanolamine in the presence of 0.2 μM URB597, and their total lipids were separated by TLC (*B*). Relative radioactivities of NAE are shown (mean values ± S.D. (*error bars*), $n = 3$) (*C*). *B*, the positions of authentic compounds on the TLC plate are indicated. *Asterisk* indicates a significant difference ($p < 0.001$).

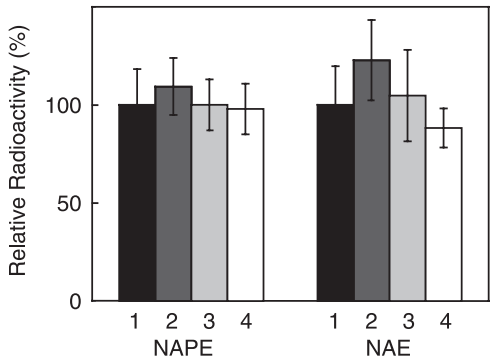

FIGURE 13. **Effects of stimulators on NAPE biosynthesis in PLA/AT-2-H cells.** PLA/AT-2-H cells were radiolabeled with [^{14}C]ethanolamine and then treated with vehicle (Me_2SO) (*lane 1*), 1 μM A23187 (*lane 2*), 10 μM forskolin (*lane 3*), or 1 μM PMA (*lane 4*) for 10 min at 37 °C. Total lipids were separated by TLC. NAPE and NAE levels of Me_2SO-treated cells are normalized to 100%, respectively, and relative radioactivities are shown (mean values ± S.D. (*error bars*), $n = 3$).

finding was fortified with the fact that brain *N*-acyltransferase (Ca-NAT) is stimulated by Ca^{2+} (15, 16). However, a certain level of NAPE appears to be present in various tissues without any cellular stimuli (2). PLA/AT-2 and other members of the PLA/AT family may thus play a role in maintaining the basal levels of NAPE. Alternatively, different from recombinant PLA/AT-2, endogenous PLA/AT-2 may be regulated by a Ca^{2+}-dependent protein.

The major *N*-acyl species of NAE in PLA/AT-2-H cells were 16:0, 18:0, and 18:1. Moreover, because the total number of double bonds in *sn*-1 *O*-acyl and *N*-acyl chains of NAPE was mostly 0 or 1, *N*-acyl species of NAPE appeared to be mostly saturated and monounsaturated acyl chains. Thus, our results using PLA/AT-2-H cells agree with the fact that NAPEs containing a saturated or monounsaturated acyl chain at the *N* position serve as precursors of bioactive saturated and monounsaturated NAEs such as *N*-palmitoylethanolamine and *N*-oleoylethanolamine. In contrast, anandamide (*N*-arachidonoylethanolamine) and its precursor *N*-arachidonoyl-PE were minor components among NAEs and NAPEs, respectively. It is well known that polyunsaturated fatty acids such as arachidonic acid are mostly esterified at the *sn*-2 position rather than *sn*-1 position of glycerophospholipids. These results are in agreement with our finding that purified PLA/AT-2 transferred an acyl chain principally from the *sn*-1 position of PC to the amino group of PE. Thus, PLA/AT-2 does not appear to be involved in a putative anandamide-specific pathway.

PLA/AT-2-H cells showed elevated levels of NAE and GP-NAE in addition to NAPE. Because GP-NAE is an intermediate metabolite generated by double deacylation of NAPE in the NAPE-PLD-independent pathway, these results suggest that NAPE generated by PLA/AT-2 is converted to NAE directly by endogenous NAPE-PLD or through the NAPE-PLD-independent pathway via GP-NAE. Transient expression of NAPE-PLD in cells caused a remarkable decrease in NAPE levels. Concomitant increases in NAE levels were observed only in the presence of URB597, which probably inhibited endogenous FAAH. Fur-

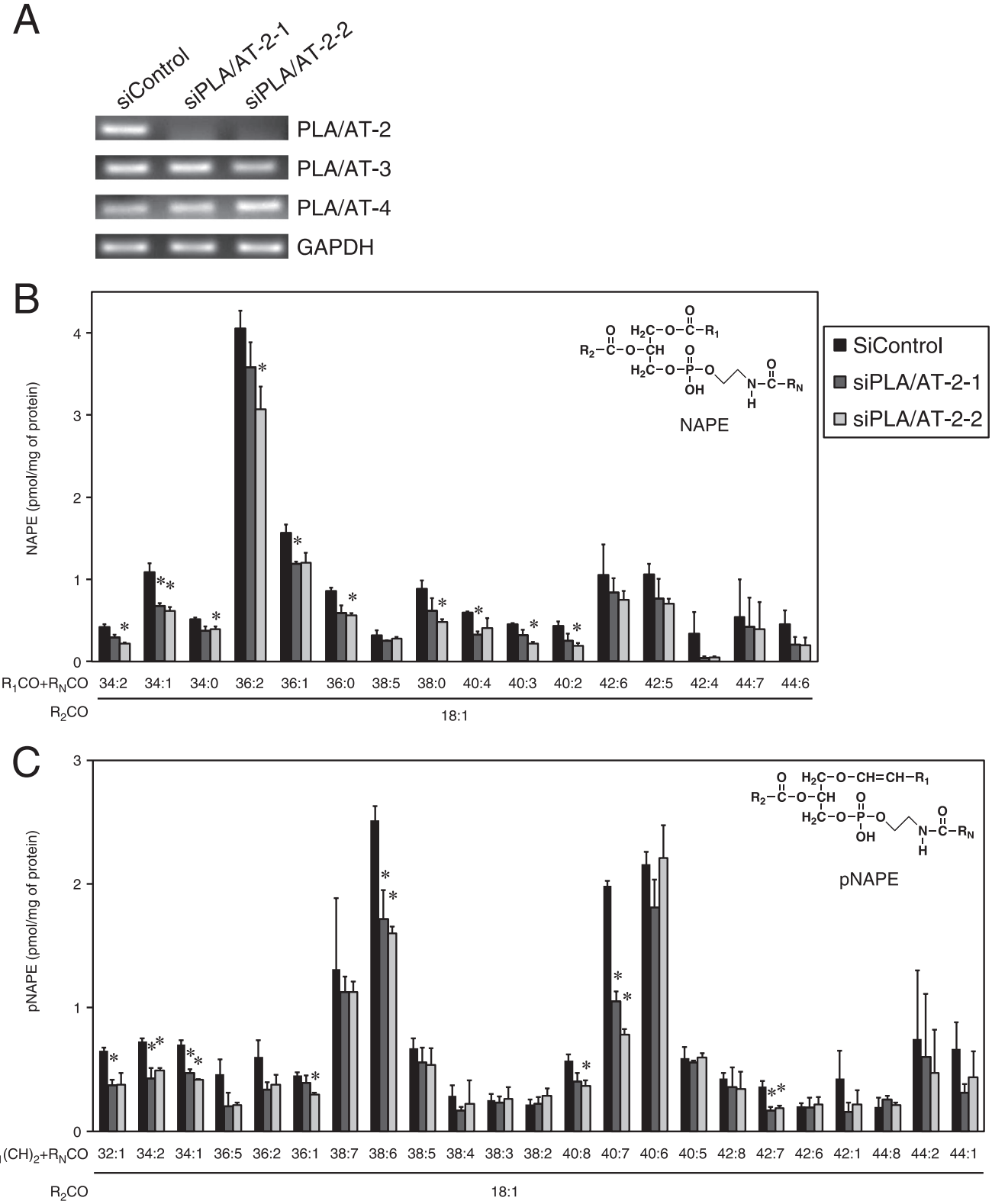

FIGURE 14. **LC-MS/MS analysis of *N*-acylated ethanolamine phospholipids in HeLa cells treated with siRNA against *PLA/AT-2*.** HeLa cells were transfected with control siRNA (*siControl*) or PLA/AT-2 siRNAs (*siPLA/AT-2–1 or -2*). After 48 h, total RNAs were isolated and analyzed by RT-PCR using specific primers for the mRNAs of PLA/AT-2–4 and GAPDH (a control) (*A*). Various species of NAPEs (*B*) and pNAPEs (*C*) in HeLa cells treated with siControl (*black*), PLA/AT-2–1 (*dark gray*), or PLA/AT-2–2 (*light gray*) were analyzed by LC-MS/MS as described under "Experimental Procedures." *N*-Heptadecanoyl-1,2-dipalmitoyl-PE was used as an internal standard. *B*, levels of pNAPEs were corrected based on the calibration line constructed with authentic *N*-heptadecanoyl-1-*O*-1′(*Z*)-octadecenyl-2-oleoyl-glycerophosphoethanolamine and *N*-heptadecanoyl-1,2-dipalmitoyl-PE. Results are shown as picomoles/mg of protein (mean values ± S.D., $n = 3$). *Asterisks* indicate significant differences from control cells ($p < 0.05$). R_1CO+R_NCO and $R_1(CH)_2+R_NCO$ represent the total number of carbon atoms and double bonds in *sn*-1 *O*-acyl (or *sn*-1 *O*-alkenyl) and *N*-acyl chains.

thermore, coexpression of NAPE-PLD and NAAA (another NAE-hydrolyzing enzyme) decreased NAE levels in URB597-treated PLA/AT-2-H cells. These results showed that exogenous NAPE-PLD was involved in the formation of NAE from NAPE produced by PLA/AT-2 and that exogenous NAAA as well as endogenous FAAH were utilized in the degradation of NAE in PLA/AT-2-H cells. Although we used only COS-7 and HEK293 cells to express PLA/AT-2, our results suggest that the introduction of the cDNA encoding *PLA/AT-2* to various types of cells serves as a useful method to examine intracellular metabolism and the actions of NAPE and NAE as well as the intracellular effects of enzyme inhibitors.

The overexpression of PLA/AT-2 also caused a decrease in the levels of plasmenylethanolamine as well as abnormal intracellular localization of peroxisomal proteins. These results suggest that overexpressed PLA/AT-2 causes the dysfunction of peroxisomes as we recently reported in PLA/AT-3-expressing cells (36). Different from PLA/AT-2, the major catalytic activity of PLA/AT-3 is $PLA_{1/2}$ activity (29, 30), and its *N*-acyltransferase activity is very low (Fig. 2). Therefore, it is unlikely that increased NAPE levels are responsible for peroxisomal dysfunction. We are now trying to elucidate a molecular mechanism underlying peroxisomal dysfunction in PLA/AT-2- and PLA/AT-3-expressing cells.

In conclusion, we demonstrated for the first time that PLA/AT-2 and other PLA/AT proteins can form NAPE in living cells. We are planning further studies, including analyses of gene-disrupted and transgenic animals for PLA/AT proteins, to elucidate their physiological significance in NAPE metabolism.

Acknowledgments—We are grateful to Akiko Yamamoto, Yumi Tani, and Ami Yamada for their technical assistance. We also acknowledge technical assistance from the Division of Research Instrument and Equipment and Division of Radioisotope Research, Kagawa University.

REFERENCES

1. Schmid, H. H. O., Schmid, P. C., and Natarajan, V. (1990) *N*-Acylated glycerophospholipids and their derivatives. *Prog. Lipid Res.* **29,** 1–43
2. Hansen, H. S., Moesgaard, B., Hansen, H. H., and Petersen, G. (2000) *N*-Acylethanolamines and precursor phospholipids. Relation to cell injury. *Chem. Phys. Lipids* **108,** 135–150
3. Devane, W. A., Hanus, L., Breuer, A., Pertwee, R. G., Stevenson, L. A., Griffin, G., Gibson, D., Mandelbaum, A., Etinger, A., and Mechoulam, R. (1992) Isolation and structure of a brain constituent that binds to the cannabinoid receptor. *Science* **258,** 1946–1949
4. Zygmunt, P. M., Petersson, J., Andersson, D. A., Chuang, H., Sørgård, M., Di Marzo, V., Julius, D., and Högestätt, E. D. (1999) Vanilloid receptors on sensory nerves mediate the vasodilator action of anandamide. *Nature* **400,** 452–457
5. Calignano, A., La Rana, G., Giuffrida, A., and Piomelli, D. (1998) Control of pain initiation by endogenous cannabinoids. *Nature* **394,** 277–281
6. Solorzano, C., Zhu, C., Battista, N., Astarita, G., Lodola, A., Rivara, S., Mor, M., Russo R, Maccarrone, M., Antonietti, F., Duranti, A., Tontini, A., Cuzzocrea, S., Tarzia, G., and Piomelli, D. (2009) Selective *N*-acylethanolamine-hydrolyzing acid amidase inhibition reveals a key role for endogenous palmitoylethanolamide in inflammation. *Proc. Natl. Acad. Sci. U.S.A.* **106,** 20966–20971
7. Rodríguez de Fonseca, F., Navarro, M., Gómez, R., Escuredo, L., Nava, F., Fu, J., Murillo-Rodríguez, E., Giuffrida, A., LoVerme, J., Gaetani, S., Kathuria, S., Gall, C., and Piomelli, D. (2001) An anorexic lipid mediator regulated by feeding. *Nature* **414,** 209–212
8. Fu, J., Gaetani, S., Oveisi, F., Lo Verme, J., Serrano, A., Rodríguez De Fonseca, F., Rosengarth, A., Luecke, H., Di Giacomo, B., Tarzia, G., and Piomelli, D. (2003) Oleylethanolamide regulates feeding and body weight through activation of the nuclear receptor PPAR-α. *Nature* **425,** 90–93
9. LoVerme, J., Russo, R., La Rana, G., Fu, J., Farthing, J., Mattace-Raso, G., Meli, R., Hohmann, A., Calignano, A., and Piomelli, D. (2006) Rapid broad spectrum analgesia through activation of peroxisome proliferator-activated receptor-α. *J. Pharmacol. Exp. Ther.* **319,** 1051–1061
10. Ahern, G. P. (2003) Activation of TRPV1 by the satiety factor oleoylethanolamide. *J. Biol. Chem.* **278,** 30429–30434
11. Overton, H. A., Babbs, A. J., Doel, S. M., Fyfe, M. C., Gardner, L. S., Griffin, G., Jackson, H. C., Procter, M. J., Rasamison, C. M., Tang-Christensen, M., Widdowson, P. S., Williams, G. M., and Reynet, C. (2006) Deorphanization of a G protein-coupled receptor for oleoylethanolamide and its use in the discovery of small molecule hypophagic agents. *Cell Metab.* **3,** 167–175
12. Ueda, N., Tsuboi, K., and Uyama, T. (2010) *N*-Acylethanolamine metabolism with special reference to *N*-acylethanolamine-hydrolyzing acid amidase (NAAA). *Prog. Lipid Res.* **49,** 299–315
13. Ueda, N., Tsuboi, K., and Uyama, T. (2010) Enzymological studies on the biosynthesis of *N*-acylethanolamines. *Biochim. Biophys. Acta* **1801,** 1274–1285
14. Cadas, H., Gaillet, S., Beltramo, M., Venance, L., and Piomelli, D. (1996) Biosynthesis of an endogenous cannabinoid precursor in neurons and its control by calcium and cAMP. *J. Neurosci.* **16,** 3934–3942
15. Cadas, H., di Tomaso, E., and Piomelli, D. (1997) Occurrence and biosynthesis of endogenous cannabinoid precursor, *N*-arachidonoylphosphatidylethanolamine, in rat brain. *J. Neurosci.* **17,** 1226–1242
16. Jin, X. H., Okamoto, Y., Morishita, J., Tsuboi, K., Tonai, T., and Ueda, N. (2007) Discovery and characterization of a Ca^{2+}-independent phosphatidylethanolamine *N*-acyltransferase generating the anandamide precursor and its congeners. *J. Biol. Chem.* **282,** 3614–3623
17. Okamoto, Y., Morishita, J., Tsuboi, K., Tonai, T., and Ueda, N. (2004) Molecular characterization of a phospholipase D generating anandamide and its congeners. *J. Biol. Chem.* **279,** 5298–5305
18. Sun, Y. X., Tsuboi, K., Okamoto, Y., Tonai, T., Murakami, M., Kudo, I., and Ueda, N. (2004) Biosynthesis of anandamide and *N*-palmitoylethanolamine by sequential actions of phospholipase A_2 and lysophospholipase D. *Biochem. J.* **380,** 749–756
19. Simon, G. M., and Cravatt, B. F. (2006) Endocannabinoid biosynthesis proceeding through glycerophospho-*N*-acylethanolamine and a role for α/β-hydrolase 4 in this pathway. *J. Biol. Chem.* **281,** 26465–26472
20. Tsuboi, K., Okamoto, Y., Ikematsu, N., Inoue, M., Shimizu, Y., Uyama, T., Wang, J., Deutsch, D. G., Burns, M. P., Ulloa, N. M., Tokumura, A., and Ueda, N. (2011) Enzymatic formation of *N*-acylethanolamines from *N*-acylethanolamine plasmalogen through *N*-acylphosphatidylethanolamine-hydrolyzing phospholipase D-dependent and -independent pathways. *Biochim. Biophys. Acta* **1811,** 565–577
21. Cravatt, B. F., Giang, D. K., Mayfield, S. P., Boger, D. L., Lerner, R. A., and Gilula, N. B. (1996) Molecular characterization of an enzyme that degrades neuromodulatory fatty acid amides. *Nature* **384,** 83–87
22. Tsuboi, K., Sun, Y. X., Okamoto, Y., Araki, N., Tonai, T., and Ueda, N. (2005) Molecular characterization of *N*-acylethanolamine-hydrolyzing acid amidase, a novel member of the choloylglycine hydrolase family with structural and functional similarity to acid ceramidase. *J. Biol. Chem.* **280,** 11082–11092
23. McKinney, M. K., and Cravatt, B. F. (2005) Structure and function of fatty acid amide hydrolase. *Annu. Rev. Biochem.* **74,** 411–432
24. Hajnal, A., Klemenz, R., and Schäfer, R. (1994) Subtraction cloning of H-rev107, a gene specifically expressed in H-ras-resistant fibroblasts. *Oncogene* **9,** 479–490
25. DiSepio, D., Ghosn, C., Eckert, R. L., Deucher, A., Robinson, N., Duvic, M., Chandraratna, R. A., and Nagpal, S. (1998) Identification and characterization of a retinoid-induced class II tumor suppressor/growth regulatory gene. *Proc. Natl. Acad. Sci. U.S.A.* **95,** 14811–14815
26. Akiyama, H., Hiraki, Y., Noda, M., Shigeno, C., Ito, H., and Nakamura, T. (1999) Molecular cloning and biological activity of a novel Ha-Ras sup-

pressor gene predominantly expressed in skeletal muscle, heart, brain, and bone marrow by differential display using clonal mouse EC cells, ATDC5. *J. Biol. Chem.* **274,** 32192–32197
27. Shyu, R. Y., Hsieh, Y. C., Tsai, F. M., Wu, C. C., and Jiang, S. Y. (2008) Cloning and functional characterization of the *HRASLS2* gene. *Amino Acids* **35,** 129–137
28. Jin, X. H., Uyama, T., Wang, J., Okamoto, Y., Tonai, T., and Ueda, N. (2009) cDNA cloning and characterization of human and mouse Ca^{2+}-independent phosphatidylethanolamine *N*-acyltransferases. *Biochim. Biophys. Acta* **1791,** 32–38
29. Uyama, T., Morishita, J., Jin, X. H., Okamoto, Y., Tsuboi, K., and Ueda, N. (2009) The tumor suppressor gene H-Rev107 functions as a novel Ca^{2+}-independent cytosolic phospholipase $A_{1/2}$ of the thiol hydrolase-type. *J. Lipid Res.* **50,** 685–693
30. Uyama, T., Jin, X. H., Tsuboi, K., Tonai, T., and Ueda, N. (2009) Characterization of the human tumor suppressors TIG3 and HRASLS2 as phospholipid-metabolizing enzymes. *Biochim. Biophys. Acta* **1791,** 1114–1124
31. Shinohara, N., Uyama, T., Jin, X. H., Tsuboi, K., Tonai, T., Houchi, H., and Ueda, N. (2011) Enzymological analysis of the tumor suppressor A-C1 reveals a novel group of phospholipid-metabolizing enzymes. *J. Lipid Res.* **52,** 1927–1935
32. Schmid, P. C., Reddy, P. V., Natarajan, V., and Schmid, H. H. O. (1983) Metabolism of *N*-acylethanolamine phospholipids by a mammalian phosphodiesterase of the phospholipase D type. *J. Biol. Chem.* **258,** 9302–9306
33. Ueda, N., Yamamoto, K., Yamamoto, S., Tokunaga, T., Shirakawa, E., Shinkai, H., Ogawa, M., Sato, T., Kudo, I., Inoue, K., Takizawa, H., Nagano, T., Hirobe, M., Matsuki, N., and Saito, H. (1995) Lipoxygenase-catalyzed oxygenation of arachidonylethanolamide, a cannabinoid receptor agonist. *Biochim. Biophys. Acta* **1254,** 127–134
34. Bligh, E. G., and Dyer, W. J. (1959) A rapid method of total lipid extraction and purification. *Can. J. Med. Sci.* **37,** 911–917
35. Okamoto, Y., Morishita, J., Wang, J., Schmid, P. C., Krebsbach, R. J., Schmid, H. H. O., and Ueda, N. (2005) Mammalian cells stably overexpressing *N*-acylphosphatidylethanolamine-hydrolyzing phospholipase D exhibit significantly decreased levels of *N*-acylphosphatidylethanolamines. *Biochem. J.* **389,** 241–247
36. Uyama, T., Ichi, I., Kono, N., Inoue, A., Tsuboi, K., Jin, X. H., Araki, N., Aoki, J., Arai, H., and Ueda, N. (2012) Regulation of peroxisomal lipid metabolism by catalytic activity of tumor suppressor H-rev107. *J. Biol. Chem.* **287,** 2706–2718
37. Luetterforst, R., Stang, E., Zorzi, N., Carozzi, A., Way, M., and Parton, R. G. (1999) Molecular characterization of caveolin association with the Golgi complex. Identification of a cis-Golgi targeting domain in the caveolin molecule. *J. Cell Biol.* **145,** 1443–1459
38. Honsho, M., Asaoku, S., and Fujiki, Y. (2010) Post-translational regulation of fatty acyl-CoA reductase 1, Far1, controls ether glycerophospholipid synthesis. *J. Biol. Chem.* **285,** 8537–8542
39. Tokumura, A., Carbone, L. D., Yoshioka, Y., Morishige, J., Kikuchi, M., Postlethwaite, A., and Watsky, M. A. (2009) Elevated serum levels of arachidonoyl-lysophosphatidic acid and sphingosine 1-phosphate in systemic sclerosis. *Int. J. Med. Sci.* **6,** 168–176
40. Chalvardjian, A., and Rudnicki, E. (1970) Determination of lipid phosphorus in the nanomolar range. *Anal. Biochem.* **36,** 225–226
41. Simon, G. M., and Cravatt, B. F. (2008) Anandamide biosynthesis catalyzed by the phosphodiesterase GDE1 and detection of glycerophospho-*N*-acylethanolamine precursors in mouse brain. *J. Biol. Chem.* **283,** 9341–9349
42. Fegley, D., Gaetani, S., Duranti, A., Tontini, A., Mor, M., Tarzia, G., and Piomelli, D. (2005) Characterization of the fatty acid amide hydrolase inhibitor cyclohexyl carbamic acid 3′-carbamoyl-biphenyl-3-yl ester (URB597). Effects on anandamide and oleoylethanolamide deactivation. *J. Pharmacol. Exp. Ther.* **313,** 352–358
43. Hansen, H. S., Lauritzen, L., Strand, A. M., Moesgaard, B., and Frandsen, A. (1995) Glutamate stimulates the formation of *N*-acylphosphatidylethanolamine and *N*-acylethanolamine in cortical neurons in culture. *Biochim. Biophys. Acta* **1258,** 303–308